Available online at www.sciencedirect.com
SCIENCE DIRECT®
PERGAMON
Continental Shelf Research 23 (2003) 1847–1875
CONTINENTAL SHELF RESEARCH
www.elsevier.com/locate/csr

Long-term simulation of main biogeochemical events in a coastal lagoon: Sacca Di Goro (Northern Adriatic Coast, Italy)

J.M. Zaldívar[a,*], E. Cattaneo[a], M. Plus[a], C.N. Murray[a], G. Giordani[b], P. Viaroli[b]

[a] *Institute for Environment and Sustainability, Inland and Marine Waters Unit, Joint Research Center, European Commission, Ispra (VA), Italy*
[b] *Dipartimento di Scienze Ambientali, Università di Parma, Parma, Italy*

Received 29 January 2002; accepted 8 January 2003

Abstract

A biogeochemical model for the Sacca di Goro Lagoon has been developed and partially validated with field data from 1989 to 1998. The model considers the nutrient cycles in the water column as well as in the sediments. Furthermore, phytoplankton, zooplankton, and *Ulva* sp. dynamics, as well as shellfish farming, are taken into account. Due to the recent anoxic crises in the lagoon, the dynamic of oxygen has also been simulated. The actual version of the model is a 0D with input fluxes from the watershed and exchange with the Northern Adriatic Sea. Nutrients from the watershed, wet and dry deposition, temperature, light intensity, wind speed and shellfish production are considered as forcing functions. The results show that the model is able to capture the essential dynamics of the lagoon, with values in the same order of magnitude with the measurements from experimental campaigns. The coupling with a 3D hydrodynamical model of the Sacca di Goro, as well as with the watershed model is presently under development.

Keywords: Ecological modelling; Biogeochemical cycles

1. Introduction

As a consequence of their location between land and sea, coastal lagoons are characterized by large fluctuations in physical and chemical conditions (Kjerfve, 1994). Moreover, coastal lagoons are subjected to strong anthropogenic pressures. They receive freshwater inputs, rich in organic and mineral nutrients derived from urban, agricultural and/or industrial effluents and domestic sewage. In addition, several of them support strong shellfish farming. Furthermore, they have been suffering from multiple and uncoordinated land-use modifications undertaken with only limited sectorial objectives in mind. For example: structural changes in lagoon topography, increase of the number of sea connections, changes in bathymetry, etc. All these factors are responsible for important disruptions in ecosystem functioning characterized by eutrophic and dystrophic conditions in summer (high temperatures 25–30°C), algal blooms, O_2 depletion and H_2S production

*Corresponding author. Fax: +39-0332-789328.
E-mail address: jose.zaldivar-comenges@jrc.it (J.M. Zaldívar).

0278-4343/$ - see front matter © 2003 Elsevier Ltd. All rights reserved.
doi:10.1016/j.csr.2003.01.001

(Pugnetti et al., 1992; Cioffi et al., 1995; Harzallah and Chapelle, 2002; amongst others).

The combination of all these different factors affecting the Mediterranean lagoons make necessary for their management, the development of management tools that are able to consider the different aspects in an integrated way. It is evident that in this case one should be able to analyse and assess lagoon fluid-dynamics, ecology, nutrients cycles, river runoff influence, shellfish farming, macroalgal blooms, as well as the economical implications of different scenario analysis.

Obviously, to carry out such a task biogeochemical models that take into account the different mechanisms and important variables in the ecosystem are fundamental (Chapelle et al., 2000; Arhonditis et al., 2000). These models are able to handle the complex link between human activities and ecosystem functioning, which are otherwise not possible to capture with more traditional statistical tools.

In this work we have, based on previously developed models (Lancelot et al., 2002; Tusseau et al., 1997; Chapelle et al., 2000; Solidoro et al., 1997a, b; Chapelle, 1995; Bacher et al., 1995), implemented and tested a biogeochemical model of the Sacca di Goro. The model considers the nutrient cycles in the water column as well as in the sediments. Furthermore, phytoplankton, zooplankton, and *Ulva* sp. dynamics, as well as shellfish farming, are taken into account. Due to the recent anoxic crises in the lagoon, the dynamic of oxygen has been also simulated. The actual version of the model is a 0D with input fluxes from the watershed and exchange with the Northern Adriatic Sea. Nutrients from the watershed, wet and dry deposition, temperature, light intensity and wind speed are considered as forcing functions.

Due to its characteristics and its economic importance, the Sacca di Goro has been the object of a continuous study and, hence, long-term data is available (Viaroli et al., 2001). We have selected to simulate the years from 1989 to 1998 for two reasons. The first is that watershed data as well as lagoon and coastal data concerning water fluxes and quality started to be monitored monthly at the end of the 80s and beginning of the 90s. The second is related to the changes and variations that Sacca di Goro has suffered during the selected period. In fact from 1987 to 1992 the Sacca di Goro experienced an abnormal proliferation of macroalgae (*Ulva rigida*), which replaced gradually phytoplankton populations (Viaroli et al., 1992). This was a clear symptom of the rapid degradation of environmental conditions and of an increase in the eutrophication of this ecosystem. The decomposition of *Ulva* in summer (high temperatures 25–30°C) produced the depletion of oxygen. At the beginning of August 1992, after a particularly severe anoxic event which resulted in a high mortality of farmed populations of mussels and clams, a channel, 300–400 m wide and more than 2 m deep, was cut through the sand bank to allow an increase in the sea water inflow and the water renewal. This measure solved temporarily the situation and in the following years a reduction of the *Ulva* cover (Viaroli et al., 1995) and an increase in phytoplankton biomass values were observed (Sei et al., 1996). However, in 1997 another anoxic event took place with half of the lagoon covered by *Ulva*, with an estimated biomass of 100–150,000 tons. The economical losses from the farmed populations of clams were around 7.5–10 million Euro (Bencivelli, 1998).

2. Study area

The Sacca di Goro (Fig. 1) is a shallow-water embayment of the Po River Delta (44.78–44.83°N, 2.25–12.33°E) approximately triangular in shape with a surface area of 26 km^2, an average depth of 1.5 m, and it is connected to the sea by two mouths about 0.9 km wide each. Numerical models (O'Kane et al., 1992) have demonstrated a clear zonation of the lagoon with the low energy eastern area separated from two higher energy zones, the western area influenced by freshwater inflow from the Po di Volano (PV) and the central area influenced by the sea. The eastern zone is very shallow (maximum depth 1 m) and accounts for one half of the total surface area and one quarter of the water volume.

The lagoon is surrounded by embankments. The main freshwater inputs are the PV River

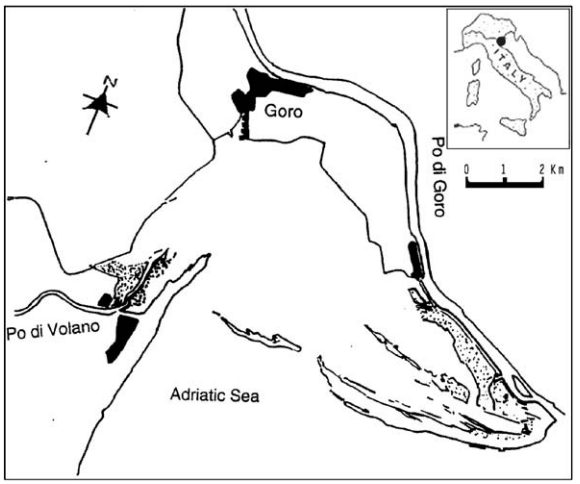

Fig. 1. General layout of the Sacca di Goro Lagoon in 1999.

($\sim 350 \times 10^6\,m^3\,yr^{-1}$), the Canal Bianco (CB) and Giralda, which have approximately the same discharge rates ($20–55 \times 10^6\,m^3\,yr^{-1}$). Freshwater inlets are also located along the Po di Goro (PG) River and are regulated by sluices. There are no direct estimates of the freshwater input from the PG, which is usually assumed to be equivalent to that of the PV. The freshwater system is mostly located in a subsident area and is regulated by a system of pumping stations (scooping plants). The fresh water or hydraulic residence time oscillates monthly between 2.5 and 122 days with a mean value of 24.5 days, whereas the water exchange time ranges from 2 to 4 days (Cattaneo et al., 2001).

The tidal amplitude is ca. 80 cm. The bottom of the lagoon is flat and the sediment is alluvial mud with high clay and silt content in the northern and central zones. Sand is more abundant near the southern shoreline, whilst sandy mud occurs in the eastern area.

The climate of the region is mediterranean with some continental influence (wet mediterranean). Precipitation is $\sim 600\,mm\,yr^{-1}$, with late spring and autumn peaks. However, this pattern is undergoing significant changes with an increase of short-term intense events.

The catchment is heavily exploited for agriculture, whilst the lagoon is one of the most important aquacultural systems in Italy. About $10\,km^2$ of the aquatic surface are exploited for farming of the Manila clam (*Tapes philippinarum*), with an annual production of about 15,000 tons. The annual revenue has been oscillating during the last few years around 50 million Euros.

In the last decade the N loading has been persistently high, about $2000\,t\,yr^{-1}$, whilst the P loading has decreased from ca. 200 to ca. $60\,t\,yr^{-1}$. The lagoon is subjected to anthropogenic eutrophication, which causes extensive growth of seaweeds, especially the chlorophyceans (*Ulva* sp. and *Cladophora* sp.) in the sheltered eastern area and phytoplankton in the deeper central zone. Macroalgal growth is responsible for summer anoxia and dystrophy, which usually take place in the eastern area (for an updated review see Viaroli et al., 2001). Recent studies have also demonstrated that the clam stock can contribute to the oxygen depletion and internal loading (Bartoli et al., 2001).

2.1. Data provision

Several data sets have been gathering from different sources, which include:

- Meteorological data concerning the PV meteorological station from Agenzia Regionale Prevenzione e Ambiente (ARPA) Bologna (http://www.regione.emilia-romagna.it/arpa/) from 1987 to 2000.
- Coastal data in the form of temperature, salinity, and nutrient concentrations was kindly provided by ARPA Cesenatico from 1984 to 1998. For this evaluation, we have mainly used data from Station 2 (Latitude: 44°47′07″, Longitude: 12°15′45″; depth: 3 m; distance from coast: 500 m), which is in front of Sacca di Goro.
- Data concerning temperature, salinity and nutrient concentrations for Sacca di Goro from 1989 and 1991 were obtained from Colombo et al. (1994) and for 1997–1998 from Milan (1999). Furthermore, long-term data concerning nutrient concentrations, oxygen and *Ulva* biomass, which has been collected during the EU funded projects ROBUST (de Wit et al., 2001) and NICE (Dalsgaard et al., 1999) has

been used to compare with simulated results. This data has been recently described in Viaroli et al. (2001).

- Data concerning fresh water entering in the Sacca di Goro (water flows and nutrient concentrations) for CB, PV and PG from 1991 to 1999 were obtained from the database of the Environment Sector in Ferrara.

3. Description of the model

Process formulations as well as relevant parameters have been taken from literature and adapted to our ecosystem. The presented model is largely based on Lancelot et al. (2002), Tusseau et al. (1997) and Chapelle et al. (2000), for the geochemical cycles and biological part. The *Ulva* sp. submodel is based on Solidoro et al. (1997a, b), whereas the sediment and oxygen was adapted from Chapelle (1995). The influence of farmed shellfish (mussels and clams) have been modified from Bacher et al. (1995).

As a first approach, we have developed a 0D version of the model, see Fig. 2. This is necessary in order to study the influence of the different parameters, to analyse the ecosystem response to changes in the initial conditions, and to investigate the importance of different parameters on the model's output.

3.1. Choice of state variables

The state space of dynamical variables considered is summarized in Table 1. We consider 38 state variables: there are 5 for nutrients in the water column and 5 in the sediments; organic matter is represented by 16 state variables in the water column and 2 in the sediments; 10 state variables represent the biological variables: six for phytoplankton, 2 for zooplankton, one for bacteria and another for *Ulva*.

Nitrogen (nitrates plus nitrites and ammonium) and phosphorous have been included into the model since these two nutrients are involved in phytoplankton growth in coastal areas. Silicate has been introduced to distinguish between diatoms and flagellates, whereas oxygen is necessary to study the evolution of hypoxia and the anoxic events that have occurred in the Sacca di Goro during the last years.

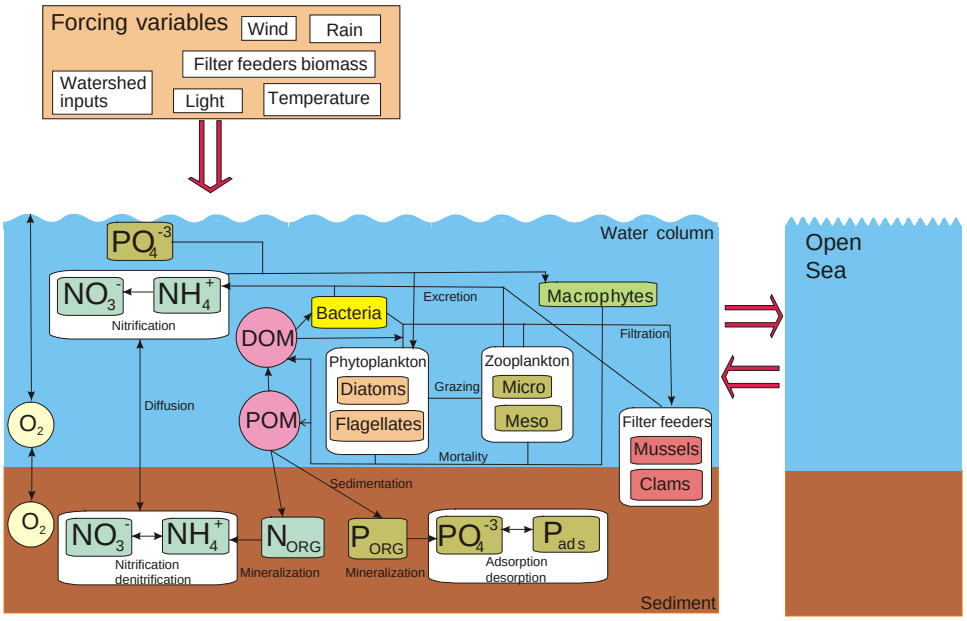

Fig. 2. General schema of the biogeochemical model for Sacca di Goro.

Table 1
State variables in the biogeochemical model

Variable name	Definition	Units
Inorganic nutrients, water column		
NO	Nitrate concentration	mmol NO^{3-}/m^3
NH	Ammonium concentration	mmol NH_4^+/m^3
PO	Reactive phosphorous concentration	mmol PO_4^{3-}/m^3
SiO	Silicate concentration	mmol $Si(OH)_4/m^3$
O	Dissolved oxygen	g O_2/m^3
Organic matter, water column		
BSC, BSN	Monomeric dissolved organic matter: carbon, nitrogen	mg C/m^3 mmol N/m^3
DC1, DN1, DP1	Dissolved polymers (high biodegradability): carbon, nitrogen, phosphorous	mg C/m^3 mmol $N\text{-}P/m^3$
DC2, DN2, DP2	Dissolved polymers (low biodegradability): carbon, nitrogen, phosphorous	mg C/m^3 mmol $N\text{-}P/m^3$
PC1, PN1, PP1	Particulate organic matter (high biodegradability): carbon, nitrogen, phosphorous	mg C/m^3 mmol $N\text{-}P/m^3$
PC2, PN2, PP2	Particulate organic matter (low biodegradability): carbon, nitrogen, phosphorous	mg C/m^3 mmol $N\text{-}P/m^3$
DSiO	Detrital biogenic silica	mmol Si/m^3
QN	Nitrogen concentration in *Ulva* tissue	mg N/gdw[a]
Biological variables, water column		
DAF, DAS, DAR	Diatoms: functional and structural metabolites, monomers, reserves	mg C/m^3
FLF, FLS, FLR	Falgellates: functional and structural metabolites, monomers, reserves	mg C/m^3
ZS	Microzooplankton density	mg C/m^3
ZL	Mesozooplankton density	mg C/m^3
B	Bacteria biomass	mg C/m^3
U	*Ulva* biomass	gdw/l
Sediments		
SNH	Ammonium concentration interstitial water	$mmol/m^3$
SNO	Nitrate concentration interstitial water	$mmol/m^3$
SPO	Phosphorous concentration interstitial water	$mmol/m^3$
SPA	Inorganic adsorbed phosphorous in sediment	μgP/g PS[b]
SO	Dissolved oxygen interstitial water	g O_2/m^3
SPP	Organic particulate phosphorous in sediment	μgP/g PS
SPN	Organic particulate nitrogen in sediment	μgN/g PS

[a] gdw is gram-dry-weight.
[b] PS stands for particulate sediment, i.e. dry sediment.

Concerning the biological components, the model, as said before, considers two types of phytoplankton and zooplankton communities, respectively. The phytoplankton model based on the AQUAPHY model (Lancelot et al., 1991) explicitly distinguishes between photosynthesis (directly dependent on irradiance) and phytoplankton growth (dependent on both nutrient and energy availability).

The microbial loop includes the release in the water column due to autolytic processes different types of organic matter: dissolved and particulate, each with two classes of biodegradability (Lancelot et al., 2002). Detrital particulate organic matter undergo sedimentation. Furthermore, the evolution of bacterial biomass is explicitly taken into account.

In shallow lagoons, sediments play an important role in biogeochemical cycles (Chapelle, 1995). The sediments have several roles: they act as sinks of organic detritus material through sedimentation; they consume oxygen due to bacterial mineralization, nitrification and benthic fauna respiration. Furthermore, they supply nutrients through remineralization of organic matter: depending on the oxygen concentration, nitrification and denitrification

takes place in sediments, and for the phosphorous the sediments act as a buffer through adsorption and desorption processes.

Ulva sp. has become an important component of the ecosystem in Sacca di Goro Lagoon. The massive presence of this macroalgae has heavily affected the Sacca di Goro ecosystem dynamics and has prompted several interventions aimed at removing its biomass in order to avoid anoxic crises, especially during the summer. In this case, apart from *Ulva* biomass, the nitrogen concentration in the macroalgae, following Solidoro et al. (1997a, b), is considered as another state variable.

Shellfish farming is implicitly taken into account through their biomass as a forcing function, and its effects on nutrients and biota through filtration, oxygen consumption and excretion that are included in the respective differential equations.

Nutrients arrive from the watershed (Burana-Po di Volano and PG) and from the airshed through wet and dry deposition, and are exchanged with the Adriatic Sea (AS). They are also exchanged with the sediments and through production by biota a fraction is converted to particulate organic matter which deposits. The cycle is closed by organic matter mineralization that occurs in the sediments.

Due to mortality or grazing, all the species produce organic matter in two forms: dissolved organic matter (DOM), which may be taken up by bacteria and particulate organic matter (POM) that deposits in the sediments, where it may be mineralized. These two compartments have also two different degradation time constants. Following Lancelot's model (2002), small zooplankton grazes flagellates and bacteria whereas large zooplankton grazes small zooplankton and diatoms. *Ulva* and phytoplankton compete for nutrients and oxygen is consumed by all species. There is a specific mortality factor for all species that depends on oxygen availability.

3.2. Model equations and parameters

The model may be divided into different submodels: phytoplankton, zooplankton, *Ulva rigida*, bacterial loop, nutrients, sediments, and shellfish. Equations and parameters are described *in extenso* in Appendix A.

3.2.1. Phytoplankton module

The phytoplankton model is mainly based on the AQUAPHY model developed by Lancelot et al. (2002) and Tusseau et al. (1997). Two functional phytoplankton groups diatoms and nanoflagellates are considered. Each phytoplanktonic community is described by three state variables defined according to their metabolic function: the monomers (S), the reserve products (R), and the functional and structural macromolecules (F).

3.2.2. Zooplankton module

The model considers two zooplankton compartments: micro-(ZS) and mesozooplankton (ZL). Feeding mechanisms of copepods (ZS and DA) and microzooplankton (B, FL) are described by a Monod-type kinetics with saturation of the specific ingestion rate at high food concentrations.

3.2.3. Ulva module

The *Ulva rigida* model has been adapted from Solidoro et al. (1997a, b). In this case the variation of *Ulva*'s biomass is expressed by the specific rates of biomass growth and losses, whereas the rate of mortality is composed of two terms (Solidoro et al., 1997a, b). The first represents the intrinsic mortality, where the second is related to the difference between the oxygen demand and the availability of dissolved oxygen.

3.2.4. Degradation of dissolved organic matter module (microbial loop)

The microbial loop model is based on the model developed in Lancelot et al. (2002), which has been adapted from the model developed by Billen (1991). In this model all organisms undergo autolytic processes which release in the water column dissolved (DOM) and particulate (POM) polymeric organic matter, each with two classes of biodegradability. In order to consider *Ulva* decomposition a specific number of terms that take into account its decomposition has been added to the original model. *Ulva* decomposition is given by $death_U$ multiplied by the corresponding parameter

depending on the element (C, N, or P) considered (in the case of N, the nitrogen *Ulva* content, *QN*, is used in the calculation instead of a constant factor). Then this quantity is divided between the different model's compartments, i.e. $ulva_{BSC}$, $ulva_{BSN}$, $ulva_{DCI}$, etc., using data from Viaroli et al. (1994). From these data, 58% of the total phosphorous from *Ulva* decomposition is released as soluble reactive phosphorous, whereas the rest is divided between organic dissolved and particulate forms. On the contrary, the percentage of nitrates and ammonium is not higher than 5% and in consequence all the *Ulva*'s nitrogen content has been divided between the organic dissolved and particulate forms.

3.2.5. Nutrients module

The nutrients included are nitrogen in the oxidized and reduced forms, phosphorous, silicate and oxygen. Phosphorus was, in principle, not considered as a limiting nutrient in Sacca di Goro (Pugnetti et al., 1992), however in order to assess the influence of different nutrients ratio and the role of the sediments in the Sacca di Goro dynamics, it has been taken into account. Furthermore, Silica has to be considered to distinguish between diatoms and flagellates and their different dynamics (Tusseau et al., 1998). Finally, in order to consider anoxic crises and to study their triggering factors, oxygen dynamics has been also simulated.

3.2.6. Sediment module

Due to the shallowness of water in Sacca di Goro, sediments play a fundamental role in understanding the nutrient dynamics (Barbanti et al., 1992; Bartoli et al., 1996). In fact, in this shallow environment, sedimentation rates of particulate matter are extremely high. Furthermore, particulate matter undergoes mineralization and through resuspension or diffusion reaches the water column. The sediment equations have been adapted from Chapelle (1995) who studied and simulated the sediment fluxes in a French Mediterranean lagoon: the Etang de Thau. In our case, as we are using a 0D model, we have considered only the first layer.

3.3. Forcing functions

Nutrients fluxes from the watershed, wet and dry deposition, temperature, light intensity, wind speed and shellfish production are considered as forcing functions.

3.3.1. Watershed

Water flows: In order to run the model, we have considered runoff fluxes from the watershed Burana-Po di Volano and from PG. The total flow from Burana-Volano (see Fig. 3a) may be obtained by adding PV and CB flows. However, an exact estimation of the water runoff entering into Sacca di Goro is difficult since we have not found data on the amount entering from PG due to the continuous changes of connections between the river and the lagoon. According to Bencivelli (private communication) a 10% of the total flow from Po river is discharged to the AS through the PG branch, and from this flow around 200–300,000 m^3/day were entering into the Sacca di Goro until 1994 when the direct connection between the Sacca and the PG was closed. This value is of the same order of magnitude of PV. After the closure in 1994 of the direct connection and the installation of sluices the flow was reduced considerably. In order to take the PG flow into account, we have considered that 5% of PG entered into the Sacca from 1989 to 1993 and after only 1% (see Fig. 3b). In this way similar values to those of PV are obtained.

Nutrient fluxes: Concerning the input of nutrients from the watershed, nitrates (plus nitrites), ammonium, phosphate, total phosphorous, reactive silica and oxygen are considered.

Nutrient inputs and outputs take into account the nutrient runoff from PV, CB and PG and the nutrient exchanged with the AS. They can be calculated as

$$Nut_{input} = \frac{F_{PV}Nut_{PV} + F_{CB}Nut_{CB} + F_{PG}Nut_{PG} + F_{AS}Nut_{AS}}{V_{SG}} + Nut_{DD} + Nut_{WD},$$

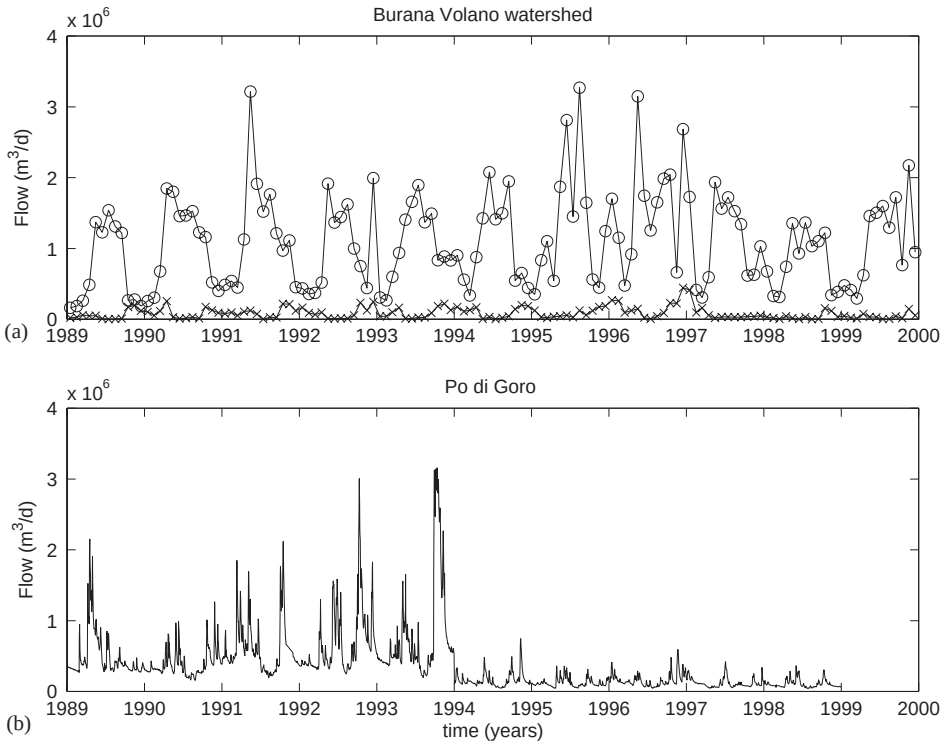

Fig. 3. Freshwater flows to Sacca di Goro (1989–1999): (a) from Burana-Volano watershed, Po di Volano(o), Canal Bianco(+)(~monthly frequency) and (b) from Po di Goro (daily frequency).

$$Nut_{output} = \frac{F_{AS} Nut_{SG}}{V_{SG}},$$

whereas F is the volumetric flow (m^3/h), Nut represents the nutrient concentration ($mmol/m^3$), V_{SG} is the total water volume in Sacca di Goro, and Nut_{DD}, Nut_{WD} represent the atmospheric nutrient fluxes from dry and wet deposition, respectively.

3.3.2. Adriatic Sea

Water flows: Water fluxes between Sacca di Goro and the AS have been obtained using the procedure recommended by Yanagi (2000), and adopted by land ocean interactions in the coastal zone (LOICZ), which consists in estimating the value of the horizontal dispersion coefficient D_H (m^2/s) by the following equation, in the case of dominant horizontal shear (wide and shallow estuarine system) recommended by Taylor (1953):

$$D_H = \frac{1}{120}\left(\frac{W^4}{K_h}\right)\left(\frac{U}{W}\right)^2,$$

where W (m) is the length of the open boundary, that is the width of the open system mouth; U (m/s) is the residual flow velocity at the surface layer of the open boundary and K_h is the horizontal diffusivity (m^2/s), which may be estimated using the following relationship (Okubo, 1971):

$$K_h = 18 W^{1.15},$$

where K_h is given in m^2/d (for LOICZ notation).

Once D_H is calculated then the water exchange flow, F_{MS}, can be evaluated using the following equation:

$$F_{MS} = D_H\left(\frac{A}{F}\right),$$

where A denotes the cross sectional area of the open boundary of the system (m^2) and F is the

Table 2
Width evolution of the Sacca di Goro mouth(s) from 1980 to 2000 (Ciavola et al., 2000)

Year	1980	1981	1982	1983	1984	1985	1986	1987	1988	1989	1990	1991	1992	1993	1994	1995	1996	1997	1998	1999	2000
W (m)	2580	2580	2580	2480	2383	2286	2189	2092	1995	1900	1700	1500	1350	1200	1284	1368	1452	1536	1626	1716	1790

Table 3
Data for the calculation of F_{AS} for the Sacca di Goro Lagoon

Variable/system	Sacca di Goro
L (m)	2270
W_{min} (m)	1200
W_{max} (m)	2580
H (m)	1.5
A_{min} (m^2)	1800
A_{max} (m^2)	3870
F (m)	4760
U (m/d)	11490[a]

[a] From Ciavola et al. (2000): mean 0.133 m/s; min. 6.0×10^{-3} m/s; max. 0.42 m/s; standard deviation 0.125 m/s.

distance (m) between the geographic center of the system and the observation point for oceanic salinity.

As the Sacca di Goro mouth has suffered several changes during the years, we have evaluated its variation during the last 20 years (Table 2) using data from Ciavola et al. (2000). During these years the principal mouth of Sacca di Goro has suffered a progressive decrease. In order to compensate this decrease a channel was opened in 1993, this channel has evolved in a second mouth ($\sim$860 m) whereas the main mouth has continued to decrease ($\sim$930 m). Table 3 shows the relative parameters used for the calculation.

Fig. 4 represents the exchange flows calculated following Yanagi (2000) procedure. The points represent the calculation based on the salinity budget, Cattaneo et al. (2001).

Nutrient fluxes: In order to evaluate the nutrients exchange with the AS, we have taken into account historical data from ARPA Station 2, which is in front of the Sacca di Goro. The model considers exchanges in oxygen, nitrogen (nitrates + nitrites and ammonium), phosphate, total phosphorous, total nitrogen and chlorophyll *a*. For the last three variables, there are specific manipulations since they have to be split into several model's compartments.

3.3.3. Atmosphere

Concerning meteorological data, total irradiance, wind speed and precipitation are introduced into the model as forcing functions. Total irradiance is used to compute the photosynthesis, wind speed is used to calculate the oxygen mass transfer rate between the atmosphere and the water column, and precipitation affects the atmospheric input of nutrients to the Sacca di Goro.

The nutrient fluxes through atmospheric wet and dry deposition have also been considered in the model in a similar procedure as described by Arhonditis et al. (2000). The estimation of these fluxes was based on existing literature for the Mediterranean (Herut and Krom, 1996; Medinets, 1996) and on local precipitation data from the meteorological station of PV for the years 1989–1998. For wet deposition, the rainfall and the mean nutrient concentration in rain water samples of: 31.1 [NO_3^-], 16.7 [NH_4^+], 0.48 [PO_4^{3-}], 1.3 [$Si(OH)_4$] mmol/m^3 were used to calculate nutrient fluxes (Herut and Krom, 1996). For dry deposition annual mean values of 110 [NO_3^-], 275 [NH_4^+], 13.9 [PO_4^{3-}] in kg/km^2·year have been used to obtain constant nutrient fluxes during the year (Medinets, 1996).

3.3.4. Biota: bivalve filter feeders

Data on bivalve filter feeders biomass have been obtained from Ceccherelli et al. (1994) and Bencivelli (private communication) and are summarized in Table 4. These values are introduced in the model assuming that shellfish farming takes place during the whole year (Ceccherelli et al., 1994). This allows to estimate the number of individuals present in the Sacca de Goro and to simulate their feeding needs in terms of nutrients and oxygen. However, shellfish biomass is treated

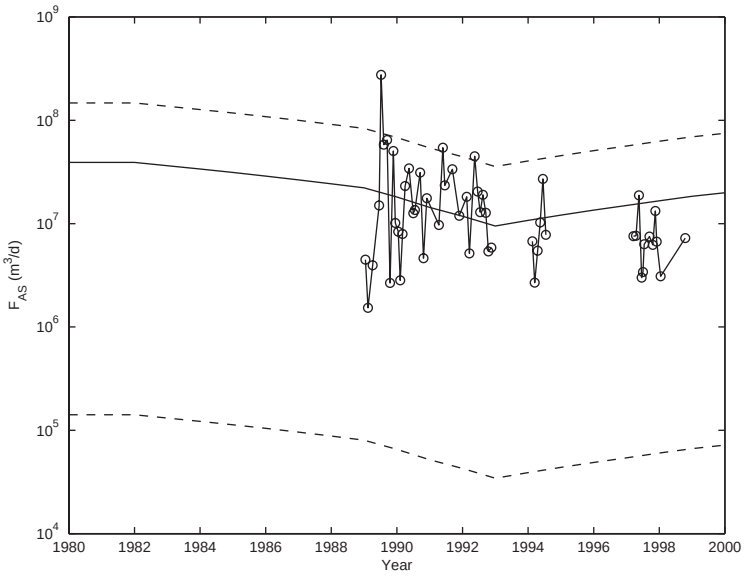

Fig. 4. Continuous line: F_{AS} calculated using the U_{mean} value from Ciavola et al. (2000). Discontinuous lines: F_{AS} calculated using the standard deviation, i.e. $U = U_{mean} \pm \Delta U$, measurements. Data points calculated using salinity budgets from LOICZ (Cattaneo et al., 2001).

Table 4
Estimation of Bivalve filter feeders (tons) in Sacca di Goro

Year	Clams[a]	Clams[b]	Mussels[b]
1987	175	35	
1988	1261	1600	
1989	4871	5300	300
1990		9300	400
1991		15500	350
1992		14300	400
1993		8500	700
1994		7000	700
1995		9000	800
1996			
1997		6000	
1998		6500–5500	
1999		6700–6500	

[a] Ceccherelli et al. (1994).
[b] Bencivelli (private communication).

as a forcing function independent of anoxic crises, or other variables that certainly would affect their life cycle. In a next step bivalve filter feeders will be introduced explicitly as a state variable(s) in the model.

The clam model was adapted from Bacher et al. (1995) and it is based on computation of the filtration, ingestion, assimilation and respiration rates as functions of the number of individuals, body dry weight, temperature and food quantity. Once these values are calculated they are introduced into the corresponding mass balances, see Appendix A.

The model has been written and implemented in FORTRAN and used a Runge–Kutta–Merson with adaptative stepsize control to solve the 38 ordinary differential equations. At each time step ($\sim$1–4 h) there is a linear interpolation to recalculate the forcing functions. A typical 10 years simulation takes $\sim$10–15 min in a Pentium III 500 MHz PC. The initial conditions of measured variables were interpolated from experimental data, whereas equilibrium was assumed between the water column and the interstitial water. This accounts for 10 variables. The others were initialised from general literature values from Sacca di Goro or similar lagoons for example, Etang de Thau for the sediments (Chapelle, 1995).

4. Results and discussion

The results of a complete 10 years simulation are summarized in Figs. 5–11. As can be seen, from

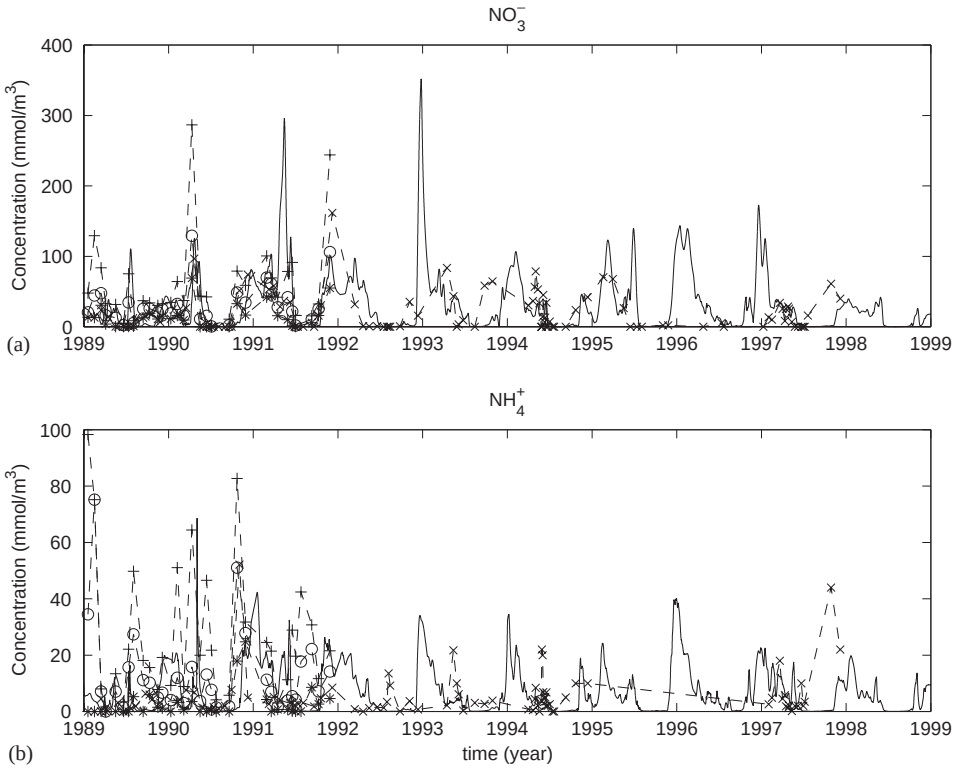

Fig. 5. Experimental (min., ×, mean, ○, and max., +, values from eight stations inside the lagoon), from Colombo et al. (1994) and from Viaroli et al. (2001) (x, Station 17 in the sheltered zone); and simulated (continuous) (a) nitrate concentrations and (b) ammonium concentrations in Sacca di Goro.

the comparison with available data, the model is able, in general terms, to capture the essential dynamics of Sacca di Goro.

The comparison between experimental and simulated nutrients is given in Figs. 5–9, whereas the mean values and standard deviation from experimental as well as for simulated values is given in Table 5. In general terms, the model shows the typical behaviour of nutrients in Sacca di Goro with an increase during autumn and winter and the subsequent depletion during spring and summer. Concerning nitrate concentrations, the peaks simulated for the model are higher than the peaks found from experimental data. This is probably produced due to the poor sampling of the values from the watershed, which are used as forcing functions. It has been seen, by comparing close measurements, that there may be a change of one order of magnitude for a particular nutrient in two successive measurements. As we are interpolating linearly between two monthly values (typical sampling time), this variability is lost and two high concentration measurements will produce a peak in the Sacca di Goro simulated concentrations since the model is considering that a large amount of nutrient is entering into the lagoon. Larger differences are found in reactive silica, for which the model predicts higher values and standard deviations. This has been also observed in Tusseau et al. (1998). This discrepancy was explained by the nutrient stoichiometric relationship chosen from phytoplankton cells, i.e. the N:Si ratio of diatoms.

Oxygen evolution in the water column is highly influenced by the anoxic crises, that occurs in the Lagoon. Experimental and simulated data are shown in Fig. 7. Oxygen concentrations in the interstitial water (Fig. 7b) are much lower than in

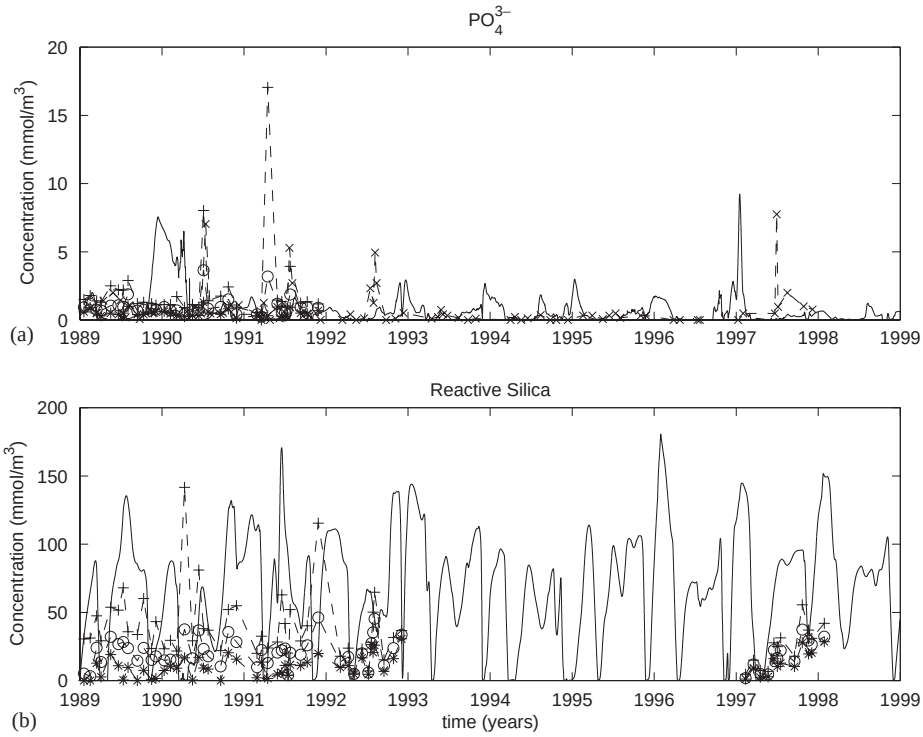

Fig. 6. Experimental (min., ×, mean, ○, and max., +, values from eight stations inside the lagoon), from Colombo et al. (1994) and from Viaroli et al. (2001) (x, Station 17 in the sheltered zone); and simulated (continuous) (a) soluble reactive phosphorous concentrations and (b) reactive silica concentrations in Sacca di Goro.

the water column. In this model only the first layer of sediment is considered. As demonstrated in Fig. 7a, the fast dynamics predicted by the model can be seen in the daily time series from the experimental data. There is no other experimental data sampled at this high frequency and hence, it is not possible to assess if the fast changes predicted by the model are in agreement with the experimental values. If this is the case, it would therefore be necessary to increase the sampling frequency, since there are a considerable number of phenomena that are lost with the typical sampling period of one week or 15 days.

Concerning the degradation of organic matter (microbial loop), there is a satisfactory agreement, in terms of general behaviour, with experimental and simulated results, see Figs. 8 and 9, for the 2 years (1991 and 1992) for which experimental data is available.

In sediments, ammonium is the major form of nitrogen in interstitial water with a mean value of 118 mmol/m^3. Nitrates are present in lower concentrations, mean value 45 mmol/m^3. Soluble reactive phosphorous concentrations are also higher in the sediment's interstitial water than in the water column, with a mean value of 7.4 mmol/m^3. The concentration of inorganic adsorbed phosphorous in the sediments decreases during anoxic crises according to the model formulation (Chapelle et al., 2000), the threshold oxygen value that triggers desorption is 0.2 g/m^3.

Phytoplankton, Fig. 10a, simulation produces similar values of chlorophyll *a*. Some of the blooms are captured by the model, however, autumnal blooms are overestimated. These blooms are produced due to the release of nutrients that follows *Ulva* decomposition. This has also been observed in Sacca di Goro, but there are also

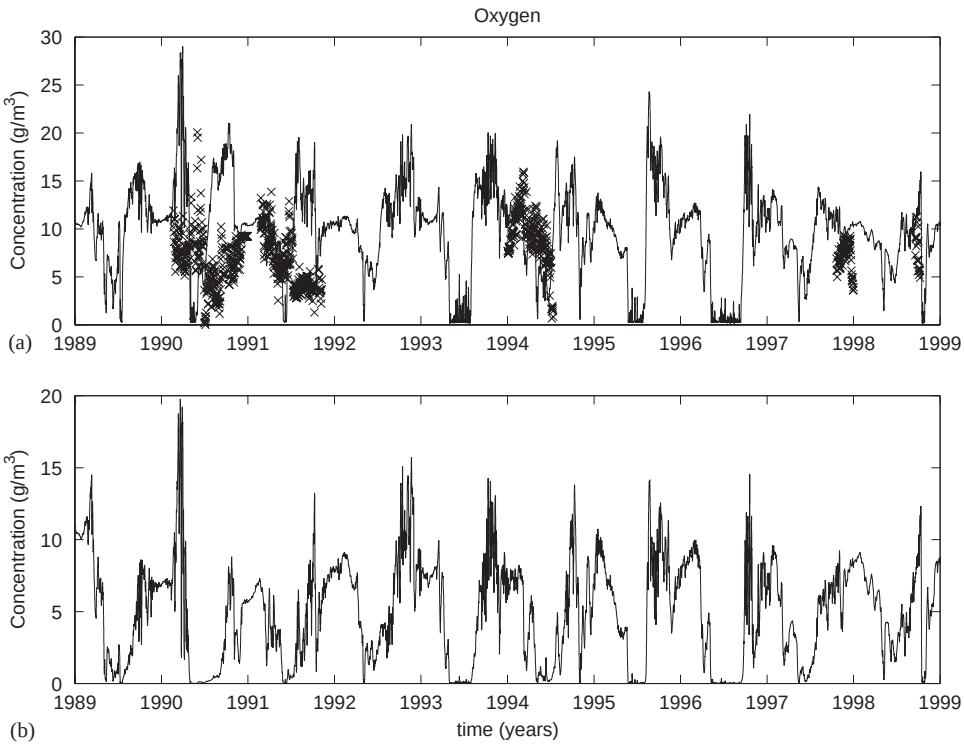

Fig. 7. Experimental (×), from the buoy from Consorzio Sacca di Goro, and simulated oxygen concentrations in: (a) the water column and (b) the interstitial water.

another macroalga that use those released nutrients (Viaroli et al., 2001).

Zooplankton and bacteria, Fig. 11, show a great variability during the simulations with several blooms during the year and high mortalities during anoxic crises. Only 1-year data for zooplankton was available and there is no data concerning bacteria, which plays an important role in consuming oxygen during anoxia.

4.1. *Ulva* and anoxic crises dynamics

Sacca di Goro has been suffering from anoxic crises during the warm season. Such crises are responsible for considerable damage to the acquaculture industry and to the ecosystem functioning. In order to individuate and verify the effectiveness of the most effective way to avoid such crises, it is important to understand the processes leading to anoxia in the lagoon. As it has been observed in Viaroli et al. (2001), the rapid growth *of Ulva* sp. in spring is followed by a decomposition process, starting from mid June. This decomposition stimulate microbial growth and produces anoxia in the water column, mostly in the bottom water. This is followed by a peak of soluble reactive phosphorous that is liberated from the sediments and from the decomposition of the macroalgal biomasses.

Fig. 10b shows the experimental and simulated *Ulva* concentrations. The model is able to predict the *Ulva* peaks and in some years their magnitude. It is clear that the *Ulva* growth has occurred in a certain area of the lagoon and the model, being 0D, is not able to take into account the spatial dimension of the problem. The simulated nitrogen content in *Ulva*, seems to follow a seasonal pattern, with high content during autumn and winter and subsequent reduction to limit values during spring, when nitrogen is depleted, in agreement with Viaroli et al. (1992).

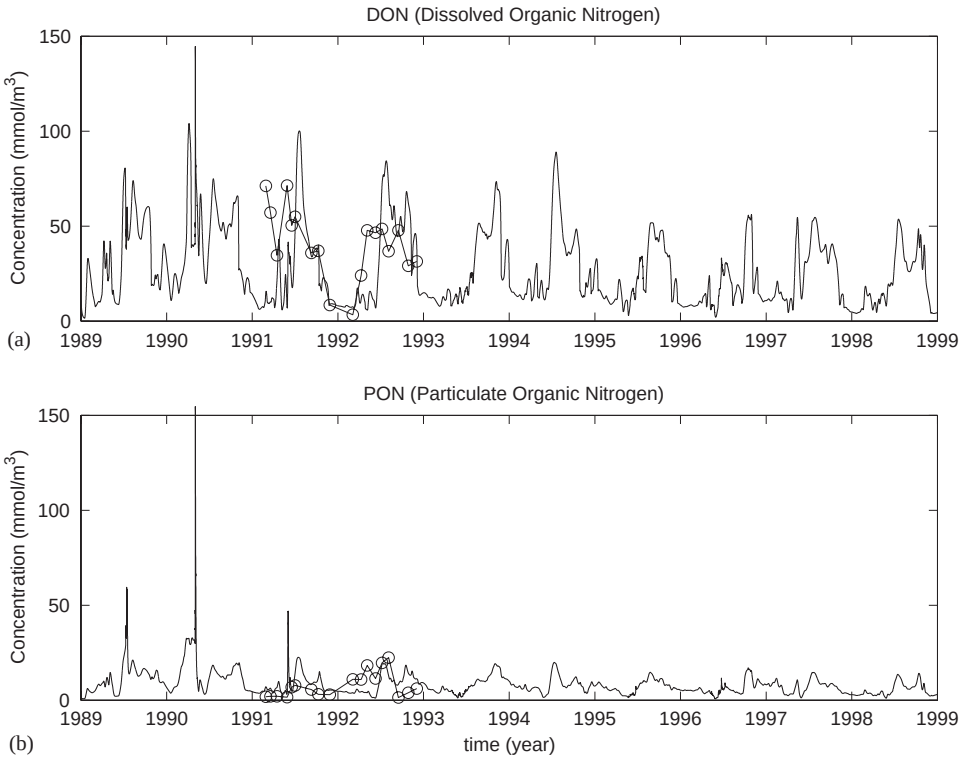

Fig. 8. Experimental, from Giordani et al. (1996) (mean value from Stations 4 and 8); and simulated (continuous) (a) dissolved organic nitrogen (DON) and (b) particulate organic nitrogen (PON) concentrations in Sacca di Goro.

Fig. 12 shows in detail the behaviour of oxygen and phosphorous as a function of *Ulva* biomass. As can be seen, when anoxia occurs there is a sudden crash of macroalgal productivity, which coincide with a significant peak in soluble reactive phosphorous due in part to the release of nutrients from *Ulva* and in part to the release of phosphorous from the sediments. Organic nutrients released by *Ulva* are used by bacteria to increase their population size producing the depletion of the oxygen available in the water column.

5. Conclusions and future developments

From the simulated results and from the comparison with available data, it seems that the model is able to capture the essential dynamics of Sacca di Goro. However, it is clear that Sacca di Goro cannot be considered as a homogeneous system, as numerous measurements campaigns have shown (Viaroli et al., 2001). Despite this, it has been necessary to carry out a 0D preliminary simulation exercise. This exercise has allowed a preliminary analysis of the influence of the forcing functions and the exchange with the boundaries, in particular the influence of the watershed, and quantifying, in a preliminary way, the magnitude of the different processes that occur in the lagoon.

The modelling results have clearly shown the necessity to reconsider the existing sampling strategies, since the time scales involved in the described processes are faster than the typical weekly or monthly data availability of most of the systems under study. This aspect makes it difficult to assess the validity of any developed model or to decide the performance of competing models. There is a need for the development of datasets that would allow a rigorous comparison between models and data so that performance of different models can be assessed and improvements can be made.

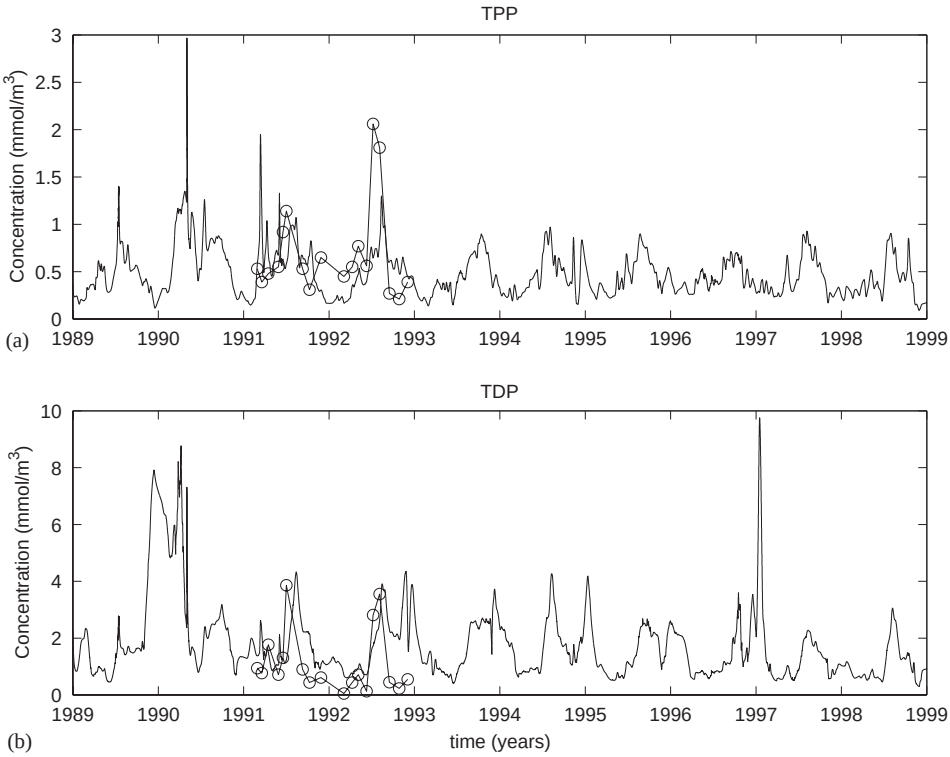

Fig. 9. Experimental, ○, from Giordani et al. (1996) (mean value from Stations 4 and 8); and simulated: (a) total particulate phosphorous (TPP) and (b) total dissolved phosphorous (TDP) in Sacca di Goro.

Another typical problem in modelling marine food webs is the extreme parametric sensitivity of the model. This means that a small change in one of the model parameters produces an important change in the simulation results. It is still not clear which part of this sensitivity is due to our lack of understanding of the ecological mechanisms that govern marine food webs, and which part is inherent to the real system and hence limits our prediction capabilities. This is an important problem that has to be addressed before deciding to use these models as management tools. We have to know what is the predictability window of our system and how accurate our forecast capabilities will be. However, despite this difficulty, it is clear that ecological modelling is becoming a mature discipline and that it is possible to couple several models with minimal modifications and obtain a coherent result for a similar test site.

The coupling with a 3D hydrodynamical model (Luyten, 1999) of the Sacca di Goro, as well as with the watershed model (Arnold et al., 1993) of Burana-Volano is presently under development. The first will allow to resolve the spatial inhomogeneities that are present in Sacca di Goro while the second will allow a better representation of the forcing functions in terms of the dynamics of nutrients arriving to Sacca di Goro, since at the moment the model is using linear interpolation between experimental data sampled every month. Due to the Sacca di Goro inhomogeneities in terms of temperature, salinity, nutrients and organisms a quantitative comparison between model results and mean values at several sampling stations will not contribute necessary to improve the model parameters. We will carry out such exercise using the 3D model when a comparison between sampling values (and not mean values for

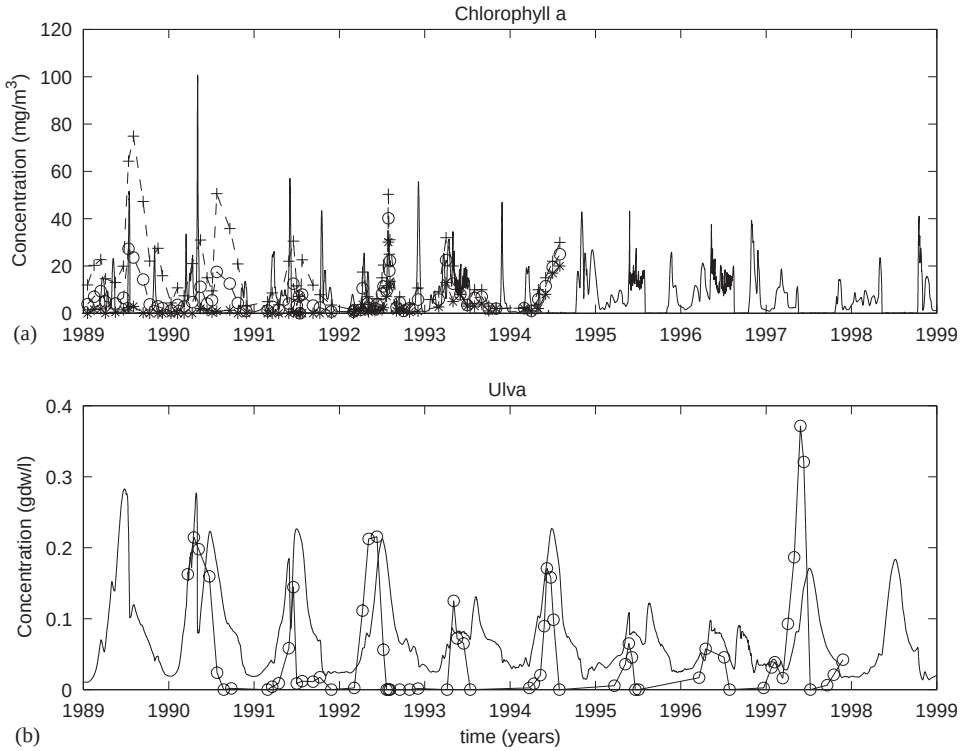

Fig. 10. (a) Experimental (min., ×, mean, ○, max., +, values from eight stations in the lagoon), from Colombo et al. (1994) and Milan (1999), and simulated (continuous) chlorophyll *a* concentrations in Sacca di Goro. (b) Experimental (○), from Viaroli et al. (2001) and Piccoli and Godini (1994) and simulated (continuous) *Ulva* biomass in Sacca di Goro.

all the lagoon) and simulated values may be carried out. Therefore, the 0D formulation can be seen as a first step in the model validation but cannot be considered as such.

Acknowledgements

We gratefully acknowledge A. Zanin, R. Martino, S. Bencivelli, and P. Magri from Assessorato Ambiente (Provincia di Ferarra) for their assistance and data provision concerning water quality. We also gratefully acknowledge G. Montanari from ARPA (Agencia Regionale Prevenzione e Ambiente) Cesenatico for data provision concerning the AS data sets. This research has been partially supported by the EU funded project DITTY (Development of Information Technology Tools for the management of European Southern lagoons under the influence of river-basin runoff) in the Energy, Environment and Sustainable Development programme of the European Commission.

Appendix A. Mathematical formulation of the model

A.1. Phytoplankton equations

The equations for diatoms are:

$$\frac{\mathrm{d}DAF}{\mathrm{d}t} = growth_D - lysis_D - grazing_D - sed,$$

$$\frac{\mathrm{d}DAS}{\mathrm{d}t} = Photosynthesis_D - storage_D + catabolism_D - growth_D - respiration_D - exudation_D - lysis_D - grazing_D - sed,$$

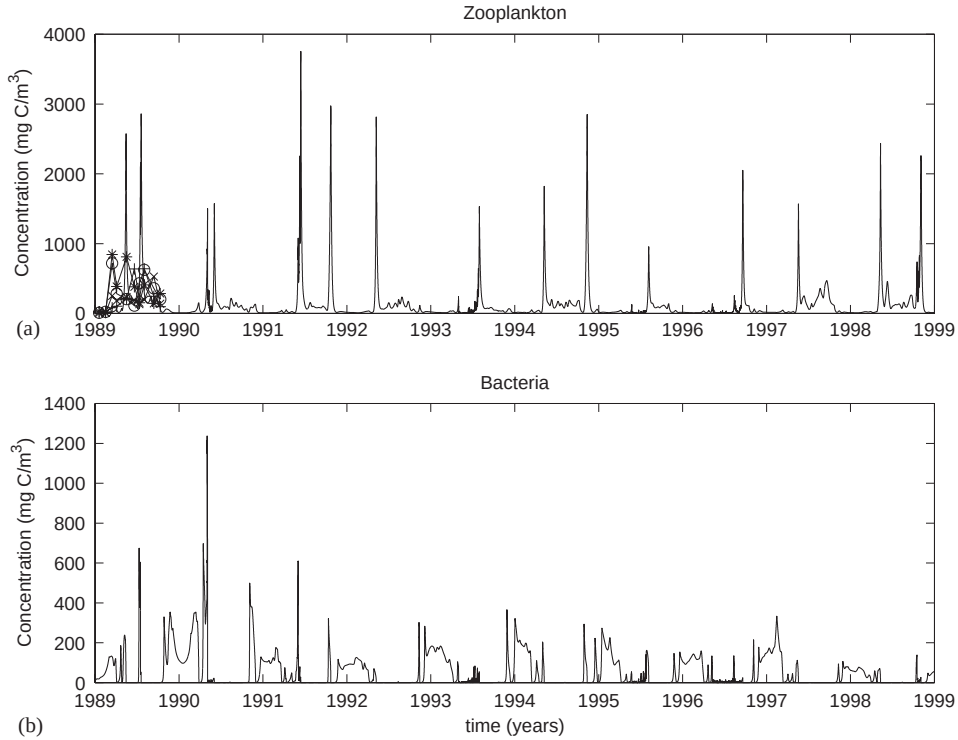

Fig. 11. (a) Experimental and simulated zooplankton values in Sacca di Goro. Experimental data for stations 1, 4, 6 and 8 from Ferrari et al. (1994). Conversion value: 1 mg C≡1000 individuals and (b) simulated bacteria biomass in Sacca di Goro.

Table 5
Mean and standard deviation over 10 years for nutrients

Nutrients	Experimental	Simulated
NO^{3-}	31.8 (37.7)	40.3 (60.5)
NH_4^+	12.1 (15.9)	11.2 (14.2)
SRP (soluble reactive phosphorous)	1.1 (1.7)	0.8 (1.3)
Reactive silica	23.7 (20.7)	68.1 (43.4)
Oxygen	7.4 (2.9)	9.9 (4.9)

$$\frac{\mathrm{d}DAR}{\mathrm{d}t} = storage_D - catabolism_D - lysis_D - grazing_D - sed.$$

Similar equations apply to the flagellates—*FLF*, *FLS*, *FLR*—but, in this case, there is no sedimentation (*sed*).

The photosynthetically active irradiance (PAR) is computed from:

$$I = I_0 \exp[-(0.0575 chl + 0.04)z],$$

where I_0 is the photosynthetically active irradiance at the surface, *chl* is chlorophyll *a* concentration (mg/m^3), $chl = (DAF + FLF)/40$ (Tusseau et al., 1998) and z is water depth (in this case $z = 0.75$ m, which is half the mean water level at Sacca di Goro).

Production due to photosynthesis can be calculated as

$$photosynthesis_D = K_{max}\left(1 - \exp\left(\frac{-\alpha I}{K_{max}}\right)\right) DAF.$$

The storage of small metabolites into reserve products is given by

$$storage_D = \rho_{max}\frac{S_{eff}}{K_{S_{eff}} + S_{eff}} DAF.$$

The reserves are catabolized according to first-order kinetics:

$$catabolism_D = k_c DAR.$$

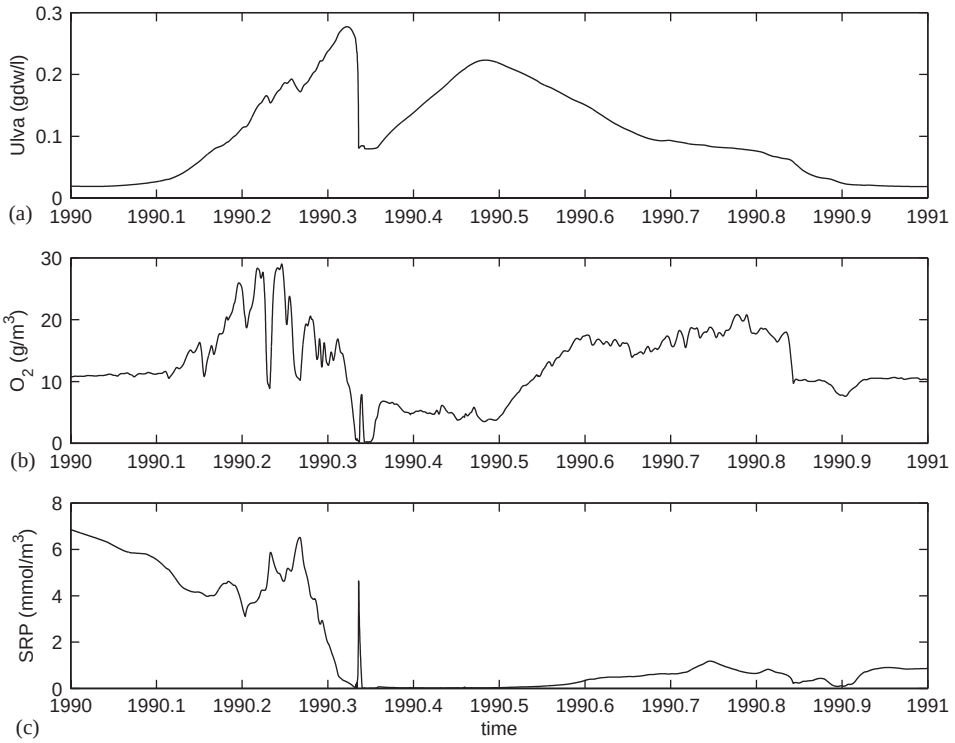

Fig. 12. Simulated 1990s anoxic crises. (a) *Ulva* biomass, (b) oxygen concentration and (c) soluble reactive phosphorous (SRP) concentration.

Growth of phytoplankton follows a Michaelis–Menten dependence of nutrient assimilation and there are two different expressions for flagellates and diatoms (with silicate as a possible limiting resource):

$$growth_F = \mu_{max} \frac{S_{eff}}{K_{S_{eff}} + S_{eff}} \min\left\{\frac{N_{tot}}{K_N + N_{tot}}, \frac{PO}{K_{PO} + PO}\right\} NFF,$$

$$growth_D = \mu_{max} \frac{S_{eff}}{K_{S_{eff}} + S_{eff}} \min\left\{\frac{SiO}{K_{Si} + SiO}, \frac{N_{tot}}{K_N + N_{tot}}, \frac{PO}{K_{PO} + PO}\right\} DAF.$$

Respiration includes several terms due to: basal respiration, motility and growth

$$respiration_D = k_m DAF + \xi\, growth_D.$$

Exudation affects only small metabolites, whereas *lysis* and sedimentation (*sed*) affects the three variables, and, hence, it is possible to write:

$$exudation_D = k_e\, photosynthesis_D,$$

$$lysis_D = k_{lys} DAX,$$

where X stand for S,F or R, respectively,

$$sed = vsed_{Dia} DAX.$$

The parameters and computed quantities to calculate the different functions are given in Table 6.

A.2. Zooplankton equations

The differential equations, which describe their population dynamics are given by

$$\frac{dZS}{dt} = growth_{ZS} - lysis_{ZS} - grazing(ZL),$$

Table 6
Parameters and computed quantities used in the phytoplankton module from Lancelot et al. (2002) and Tusseau et al. (1997)

Parameters, computed quantities	Description	Diatoms	Flagellates
K_{max}	Maximum rate of photosynthesis, $K_{max} = K'_{max}\exp\left[-\left(\frac{T-T_{opt}}{T_{width}}\right)^2\right]$		
K'_{max}	Maximum rate of photosynthesis at optimal temperature	$0.25\,h^{-1}$	$0.23\,h^{-1}$
α	Photosynthetic efficiency $(\mu Em^{-2}s^{-1})^{-1}\,h^{-1}$	0.0014	0.0016
ρ_{max}	Maximum storage rate, $\rho_{max} = \rho'_{max}\exp\left[-\left(\frac{T-T_{opt}}{T_{width}}\right)^2\right]$		
ρ'_{max}	Maximal rate of reserve synthesis	$0.23\,h^{-1}$	$0.23\,h^{-1}$
S_{eff}	Excess of S/F regarding the cellular quota Q_S, S_{eff}=(DAS/DAF)		
$K_{S_{eff}}$	Half-saturation constant regarding S_{eff} (dimensionless)	0.075	0.0075
μ_{max}	Maximum growth rate, $\mu_{max} = \mu'_{max}\exp\left[-\left(\frac{T-T_{opt}}{T_{width}}\right)^2\right]$		
μ'_{max}	Maximum growth rate at optimal temperature	$0.052\,h^{-1}$	$0.052\,h^{-1}$
T_{opt}	Optimal temperature	13.5°C	20°C
T_{width}	Sigmoid width	2.5°C	7.5°C
N_{tot}	Total nitrogen concentration, $N_{tot} = NO{+}NH$		
K_N	Half-saturation constant regarding total nitrogen	$1.2\,mmol/m^3$	$0.8\,mmol/m^3$
K_{PO}	Half-saturation constant regarding phosphorous	$0.1\,mmol/m^3$	$0.02\,mmol/m^3$
K_{Si}	Half-saturation constant regarding silica	$1.0\,mmol/m^3$	—
k_m	Maintenance constant	$0.0003\,h^{-1}$	$0.0005\,h^{-1}$
ξ	Biosynthesis cost, $\xi = 0.4rpi + 0.8(1 - rpi)$		
rpi	Ammonium preference, $rpi = \alpha_{rpi}\frac{NH}{N_{tot}}$		
α_{rpi}	Relative preference index	0.3	0.4
k_c	Rate of reserves catabolism, $k_c = k'_c\exp\left[-\left(\frac{T-T_{opt}}{T_{width}}\right)^2\right]$		
k'_c	Catabolism rate constant	$0.06\,h^{-1}$	$0.06\,h^{-1}$
k_e	Exudation rate constant	$0.005\,h^{-1}$	$0.005\,h^{-1}$
k_{lys}	Lysis rate constant	$0.0005\,h^{-1}$	$0.002\,h^{-1}$
$vsed_{Dia}$	Diatoms sedimentation rate	0.008 m/h	—
CN_P	Phytoplankton stoichiometry C/N (mg C (F)/mmol N)	48.0	48.0
CP_P	Phytoplankton stoichiometry C/P (mg C (F)/mmol P)	960.0	960.0
CSi_P	Phytoplankton stoichiometry C/Si (mg C (F)/mmol Si)	39.2	—

$$\frac{dZL}{dt} = growth_{ZL} - lysis_{ZL} - egestion.$$

The specific ingestion rate of ZL and ZS on a given prey P_i ($P_i = B$ and FL for ZL, and DA and ZS for ZL) is described by

$$grazing_i = g_{max}\frac{P_i}{P_i + K_i^{app}}G$$

with

$$K_i^{app} = K_i\left(1 + \sum_{j(\neq i)}^{n}\frac{P_j}{K_j}\right),$$

where K_i^{app} is the apparent half-saturation constant of grazing on prey i, K_j is the half saturation constant of grazing on prey j, g_{max} is the maximum specific ingestion rate, P_i is the concentration of prey i and G is the grazer concentration. Growth and egestion, in this case, are defined as a percentage (Y, E_Z) of the grazing, i.e. $growth = Y\,grazing$ and $eggestion\ eg_{ZL} = E_Z\,grazing$, whereas mortality ($lysis$) is linearly related with the prey concentration, i.e. $lysis = k_d ZX$.

The parameters and computed quantities to calculate the different functions are given in Table 7.

Table 7
Parameters and computed quantities used in the zooplankton model, from Lancelot et al. (2002)

Parameters, computed quantities	Description	Microzooplankton	Mesozooplankton
g_{max}	Maximum grazing rate, $g_{max} = g'_{max}\exp\left[-\left(\frac{T-T_{opt}}{T_{width}}\right)^2\right]$		
g'_{max}	Grazing rate at optimal temperature	$0.10\,h^{-1}$	$0.12\,h^{-1}$
T_{opt}	Optimal temperature	23°C	23°C
T_{width}	Sigmoid width	12°C	8°C
K_B	Half-saturation on bacteria	$15\,mg\,C/m^3$	—
K_{FL}	Half-saturation on flagellates	$10\,mg\,C/m^3$	—
K_{DA}	Half-saturation on diatoms	—	$50\,mg\,C/m^3$
K_{ZS}	Half-saturation on microzooplankton	—	$25\,mg\,C/m^3$
Y	Growth efficiency	0.3	0.33
k_d	Mortality constant	$0.003\,h^{-1}$	$0.001\,h^{-1}$
E_Z	Egestion constant	—	0.25
CN_Z	Ratio carbon/nitrogen (mg C/mmol N)	63.0	63.0
NP_Z	Ratio nitrogen/phosphorous (mmol N/mmol P)	16.0	16.0

A.3. Ulva equations

$$\frac{dU}{dt} = growth_U - death_U.$$

The influence of the limiting factors on *Ulva* growth was described with a multiplicative formulation:

$$growth_U = \mu(I, T, QN, PO)U,$$

whereas

$$\mu = \mu_{max} f_1(I) f_2(T) f_3(QN) f_4(PO).$$

The functional forms of the algae model are described in Table 8.

The mortality terms can be expressed as

$$death_U = k_d U^{\beta} + k_t \frac{\max[(f_{resp}U - O), 0]}{f_{resp}U}.$$

As *Ulva* is able to store nitrogen, Solidoro et al. (1997) introduced the tissue concentration of this element (QN) as a separated state variable. Its dynamics can be expressed as

$$\frac{dQN}{dt} = T_{SU} - \mu QN.$$

The specific uptake rate of nitrogen depends on the chemical form available and on the level QN of nitrogen tissue concentration. Hence, T_{SU} can be written as

$$T_{SU} = T_{SUNH} + T_{SUNO},$$

whereas

$$T_{SUNH} = V_{NH} \frac{NH}{k_{NH} + NH} \frac{QN_{max} - QN}{QN_{max} - QN_{min}}$$

and

$$T_{SUNO} = V_{NO} \frac{NO}{k_{NO} + NO} \frac{QN_{max} - QN}{QN_{max} - QN_{min}}.$$

A.4. Degradation of dissolved organic matter equations (microbial loop)

The bacteria biomass (B) dynamics may be expressed as (Table 9)

$$\frac{dB}{dt} = growth_B - lysis_B - grazing(ZS),$$

whereas bacterial growth represents a fraction of the monomers (BSC and BSN) uptake, i.e. $growth_B = Y_B upt_B$, and bacterial uptake is defined as

$$upt_B = b_{max} \frac{BSC}{K_{BSC} + BSC} B + b_{max} \frac{BSN}{K_{BSN} + BSN} B.$$

Bacterial lysis is defined as: $lysis_B = kd_B B$. Concerning the dynamics of dissolved organic matter (DOM) and particulate organic matter (POM), the

Table 8
Parameters and computed quantities used in the *Ulva* model from Solidoro et al. (1997a, b)

Parameters, computed quantities	Description	Value
μ_{max}	Maximum specific growth	$0.01875\,h^{-1}$
$f_1(I)$	$f_1(I) = 1 - \exp(-I/I_s)$ $I = I_0\exp[-(0.0575chl + 20.0U + 0.04)z]$	
I_S	Photosynthetic efficiency parameter	$60.0\,\mu Em^{-2}s^{-1}$
$f_2(T)$	$f_2(T) = \frac{1}{1+\exp(-\varsigma(T-T_U))}$	
ζ	Temperature coefficient	$0.2^\circ C^{-1}$
T_U	Temperature reference	$12.5^\circ C$
$f_3(QN)$	$f_3(QN) = \frac{QN - QN_{min}}{QN - k_{lc}}$	
QN_{min}	Min. value for N quota	10.0 mg N/gdw
QN_{max}	Max. value for N quota	42.0 mg N/gdw
k_{lc}	Critical N quota level	7.0 mg N/gdw
$f_4(PO)$	$f_4(PO) = \frac{PO}{PO + k_{up}}$	
k_{up}	Half-saturation for phosphorous	$0.323\,mmol/m^3$
$f_{resp}(T)$	$f_{resp}(T) = \frac{1}{1+\exp[-\varsigma_{resp}(T-T_{resp})]}$	
ζ_{resp}	Temperature coefficient	$0.3^\circ C^{-1}$
T_{resp}	Temperature reference	$10.0^\circ C$
k_d	Mortality rate	$0.085\,h^{-1}$
β	Coefficient in the intrinsic mortality expression	0.84
k_t	Mortality rate due to oxygen deficiency	$5.0\,h^{-1}$
V_{NH}	Max. specific uptake rate for ammonium (mg N/gdw h)	8.5
V_{NO}	Max. specific uptake rate for nitrate (mg N/gdw h)	0.45
k_{NH}	Half-saturation for ammonium	$7.14\,mmol/m^3$
k_{NO}	Half-saturation for nitrate	$3.57\,mmol/m^3$

following equations are used:

(a) *Monomeric organic matter (BSC, BSN)*

$$\frac{dBSC}{dt} = elys_{DC1} + elys_{DC2} + lys_{DAS} + lys_{FLS} + e_{DAS} + e_{FLS} - upt_B^{BSC} + ulva_{BSC} - BSC_{output},$$

$$\frac{dBSN}{dt} = elys_{DC1}\frac{DN1}{DC1} + elys_{DC2}\frac{DN2}{DC2} - upt_B^{BSN} + ulva_{BSN} + BSN_{input} - BSN_{output},$$

whereas *elys* refers to the exoenzymatic hydrolysis of $DC1$ and $DC2$ (Lancelot et al., 2002) which is expressed as

$$elys_{DCi} = ke_i\frac{DCi}{Kh_i + DCi} \quad \text{for } i = 1 \text{ and } 2.$$

(b) *Dissolved polymers high and low biodegradability, carbon (DC1, DC2)*

$$\frac{dDC1}{dt} = \varepsilon_{d1}lys_{BIO} + \gamma_{d1}eg_{ZL} - elys_{DC1} + elys_{PC1} + ulva_{DC1} - DC1_{output},$$

$$\frac{dDC2}{dt} = \varepsilon_{d2}lys_{BIO} + \gamma_{d2}eg_{ZL} - elys_{DC2} + elys_{PC2} + ulva_{DC2} - DC2_{output},$$

whereas lys_{BIO} can be obtained as

$$lys_{BIO} = lys_{DAF} + lys_{DAR} + lys_{FLF} + lys_{FLR} + lys_{BAC} + lys_{ZS} + lys_{ZL}$$

and *elys* refers to the ectoenzymatic hydrolysis:

$$elys_{PCi} = kb_iPCi \quad \text{for } i = 1 \text{ and } 2.$$

Table 9
Parameters and computed quantities used in the microbial loop model, from Lancelot et al. (2002)

Parameters, computed quantities	Description	Value
Y_B	Bacteria growth efficiency	0.3
b_{max}	Maximum rate of bacterial uptake, $b_{max} = b'_{max}\exp\left[-\left(\frac{T - T_{opt}}{T_{width}}\right)^2\right]$	
b'_{max}	Maximum rate at optimal temperature	$0.4\,h^{-1}$
T_{opt}	Optimal temperature	$30.0^{\circ}C$
T_{width}	Sigmoid width	$18^{\circ}C$
K_{BSC}	Maximum hydrolysis rate, $h_{max} = h'_{max}\exp\left[-\left(\frac{T - T_{opt}}{T_{width}}\right)^2\right]$	
K_{BSN}	Maximum rate of hydrolysis at optimal temperature	$0.6\,h^{-1}$
K_{BSC}	Half-saturation constant regarding the uptake of BSC	$25\,mg\,C/m^3$
K_{BSN}	Half-saturation constant regarding the uptake of BSN (K_{BSC}/CN)	$6.25\,mm\,N/m^3$
kd_B	Bacterial lysis rate constant	$0.01\,h^{-1}$
ke_i	Max. rate of DCi ($i = 1$ or 2) hydrolysis, $ke_i = ke'_{max}\exp\left[-\left(\frac{T - T_{opt}}{T_{width}}\right)^2\right]$	
ke'_1	Maximum rate of DC1 hydrolysis at optimal temperature	$0.75\,h^{-1}$
ke'_2	Maximum rate of DC2 hydrolysis at optimal temperature	$0.25\,h^{-1}$
Kh_1	Half-saturation constant for DC1 hydrolysis	$250\,mg\,C/m^3$
Kh_2	Half-saturation constant for DC2 hydrolysis	$2500\,mg\,C/m^3$
ε_{d1}	DC1 fraction in lysis products	0.3
ε_{d2}	DC2 fraction in lysis products	0.2
γ_{d1}	DC1 fraction in eggestion	0.1
γ_{d2}	DC2 fraction in eggestion	0.2
kb_i	Max. rate of PCi ($i = 1$ or 2) hydrolysis, $kb_i = kb'_{max}\exp\left[-\left(\frac{T - T_{opt}}{T_{width}}\right)^2\right]$	
kb'_1	Maximum rate of PC1 hydrolysis at optimal temperature	$0.005\,h^{-1}$
kb'_2	Maximum rate of PC2 hydrolysis at optimal temperature	$0.00025\,h^{-1}$
ε_{p1}	PC1 fraction in lysis products	0.1
ε_{p2}	PC2 fraction in lysis products	0.4
γ_{p1}	PC1 fraction in eggestion	0.3
γ_{p2}	PC2 fraction in eggestion	0.4
$vsed_P$	Sedimentation rate for particulate organic matter (POM)	$0.013\,h^{-1}$
CN_B	Bacterial C/N ratio (mg C/mmol N)	48
CP_B	Bacterial C/P ratio (mg C/mmol P)	1272
R_{UPC}	*Ulva*'s P stoichiometric ratio	$2.5\,mg\,P/gdw$
η_{bsc}	BSC fraction in *Ulva* lysis products	0.2
η_{dc1}	DC1 fraction in *Ulva* lysis products	0.2
η_{dc2}	DC2 fraction in *Ulva* lysis products	0.2
η_{pc1}	PC1 fraction in *Ulva* lysis products	0.2
η_{pc2}	PC2 fraction in *Ulva* lysis products	0.2
φ_{bsn}	BSN fraction in *Ulva* lysis products	0.3
φ_{dn1}	DN1 fraction in *Ulva* lysis products	0.1
φ_{dn2}	DN2 fraction in *Ulva* lysis products	0.2
φ_{pn1}	PN1 fraction in *Ulva* lysis products	0.2
φ_{pn2}	PN2 fraction in *Ulva* lysis products	0.2
κ_{po}	PO fraction in *Ulva* lysis products	0.6
κ_{dn1}	DP1 fraction in *Ulva* lysis products	0.1
κ_{dn2}	DP2 fraction in *Ulva* lysis products	0.1
κ_{pn1}	PP1 fraction in *Ulva* lysis products	0.1
κ_{pn2}	PP2 fraction in *Ulva* lysis products	0.1

(c) *Particulate organic matter high and low biodegradability, carbon (PC1, PC2)*

$$\frac{dPC1}{dt} = \varepsilon_{p1} lys_{BIO} + \gamma_{p1} eg_{ZL} - elys_{PC1} - sed_{PC1} + ulva_{PC1} - PC1_{output},$$

$$\frac{dPC2}{dt} = \varepsilon_{p2} lys_{BIO} + \gamma_{p2} eg_{ZL} - elys_{PC2} - sed_{PC2} + ulva_{PC2} - PC2_{output},$$

whereas the sedimentation of POM is defined as: $sed_{PCi} = vsed_P PCi$ for $i = 1$ and 2.

(d) *Dissolved polymers high and low biodegradability, nitrogen (DN1, DN2)*

$$\frac{dDN1}{dt} = \varepsilon_{d1} lysN_{BIO} + \gamma_{d1} \frac{eg_{ZL}}{CN_Z} - elys_{DC1} \frac{DN1}{DC1} + elys_{PN1} + ulva_{DN1} + DN1_{input} - DN1_{output},$$

$$\frac{dDN2}{dt} = \varepsilon_{d2} lysN_{BIO} + \gamma_{d2} \frac{eg_{ZL}}{CN_Z} - elys_{DC2} \frac{DN2}{DC2} + elys_{PN2} + ulva_{DN2} + DN2_{input} - DN2_{output},$$

whereas $lysN_{BIO}$ can be obtained as

$$lysN_{BIO} = \frac{lys_{DAF} + lys_{DAR} + lys_{FLF} + lys_{FLR}}{CN_P} + \frac{lys_B}{CN_B} + \frac{lys_{ZS} + lys_{ZL}}{CN_Z}.$$

(e) *Particulate organic matter high and low biodegradability, nitrogen (PN1, PN2)*

$$\frac{dPN1}{dt} = \varepsilon_{p1} lysN_{BIO} + \gamma_{p1} \frac{eg_{ZL}}{CN_Z} - elys_{PN1} - sed_{PN1} + ulva_{PN1} + PN1_{input} - PN1_{output},$$

$$\frac{dPN2}{dt} = \varepsilon_{p2} lysN_{BIO} + \gamma_{p2} \frac{eg_{ZL}}{CN_Z} - elys_{PN2} - sed_{PN2} + ulva_{PN2} + PN2_{input} - PN2_{output}.$$

(f) *Dissolved polymers high and low biodegradability, phosphorous (DP1, DP2)*

$$\frac{dDP1}{dt} = \varepsilon_{d1} lysP_{BIO} + \gamma_{d1} \frac{eg_{ZL}}{CP_Z} - elys_{DC1} \frac{DP1}{DC1} + elys_{PP1} + ulva_{DP1} + DP1_{input} - DP1_{output},$$

$$\frac{dDP2}{dt} = \varepsilon_{d2} lysP_{BIO} + \gamma_{d2} \frac{eg_{ZL}}{CP_Z} - elys_{DC2} \frac{DP1}{DC1} + elys_{PP2} + ulva_{DP2} + DP2_{input} - DP2_{output},$$

whereas $lysP_{BIO}$ can be obtained as

$$lysP_{BIO} = \frac{lys_{DAF} + lys_{DAR} + lys_{FLF} + lys_{FLR}}{CP_P} + \frac{lys_B}{CP_B} + \frac{lys_{ZS} + lys_{ZL}}{CP_Z}.$$

(g) *Particulate organic matter high and low biodegradability, phosphorous (PP1, PP2)*

$$\frac{dPP1}{dt} = \varepsilon_{p1} lysP_{BIO} + \gamma_{p1} \frac{eg_{ZL}}{CP_Z} - elys_{PP1} - sed_{PP1} + ulva_{PP1} + PP1_{input} - PP1_{output},$$

$$\frac{dPP2}{dt} = \varepsilon_{p2} lysP_{BIO} + \gamma_{p2} \frac{eg_{ZL}}{CP_Z} - elys_{PP2} - sed_{PP2} + ulva_{PP2} + PP2_{input} - PP2_{output}.$$

A.5. Nutrients equations

(a) *Dissolved inorganic nitrogen (DIN)*

$$\frac{dNO}{dt} = Nitrif_W - upt_{NO} + \frac{NO_{diffus}}{watervol} + NO_{input} - NO_{output},$$

$$\frac{dNH}{dt} = -Nitrif_W - upt_{NH} + reg_{NH} + \frac{NH_{diffus}}{watervol} + NH_{input} - NH_{output}.$$

Nitrification rates in the water column are functions of water temperature and oxygen concentration, and they can be expressed as

$$Nnitrif_W = k_{nit} f_1(T) f_2(O) NH.$$

NO uptake ($mmol\,N/m^3\,h$) can be divided into phytoplankton uptake and *Ulva* uptake ($upt_{NO} = upt_{NOPHY} + upt_{NOU}$):

$$upt_{NOPHY} = (1 - rpi_D) \frac{growth_{DA}}{CN_P} + (1 - rpi_F) \frac{growth_{NF}}{CN_P},$$

$$upt_{NOU} = \alpha_1 T_{SUNO} U,$$

whereas α_1 is a conversion factor to pass from mg N to mmol N. NH uptake (mmol N/m^3 h) can be divided into phytoplankton uptake and *Ulva* uptake (upt_{NH}=upt_{NHPHY}+upt_{NHU}).

$$upt_{NHPHY} = rpi_D \frac{growth_{DA}}{CN_P} + rpi_F \frac{growth_{NF}}{CN_P},$$

$$upt_{NHU} = \alpha_2 T_{SUNH} U,$$

whereas α_2 is a conversion factor to pass from mg N to mmol N.

The ammonification process is due to bacteria, zooplankton and shellfish, and can be represented by

$$reg_{NH} = reg_B + reg_{ZS} + reg_{ZL} + reg_{SF},$$

$$reg_B = \frac{1 - Y_B}{Y_B} \frac{upt_B}{CN_B}, \quad reg_{ZS} = \frac{1 - Y_{ZS}}{Y_{ZS}} \frac{growth_{ZS}}{CN_Z},$$
$$reg_{ZL} = \frac{1 - Y_{ZL}}{Y_{ZL}} \frac{growth_{ZL}}{CN_Z}.$$

(b) *Soluble reactive phosphorous (SRP)*

$$\frac{dPO}{dt} = -upt_{PO} + \frac{PO_{diffus}}{watervol} + elys_{DC1} \frac{DP1}{DC1} + elys_{PC1} \frac{PP1}{PC1} + ulva_{PO} + PO_{input} - PO_{output}.$$

PO uptake (mmol P/m^3 h) can be divided into phytoplankton uptake and *Ulva* uptake (upt_{PO}=upt_{POPHY}+upt_{POU})

$$upt_{POPHY} = \frac{growth_{DA}}{CP_P} + \frac{growth_{NF}}{CP_P},$$

$$upt_{POU} = \alpha_3 R_{UPC} growth_U,$$

whereas α_3 is a conversion factor to pass from mg P to mmol P.

(c) *Silica and detrital biogenic silica*

The mass balance of silica can be written as

$$\frac{dSiO}{dt} = -upt_{SiO} + k_{DSiO} DSiO + SiO_{input} - SiO_{output},$$

whereas upt_{SiO} refers to the silicate uptake by diatoms and may be expressed as

$$upt_{SiO} = \frac{growth_{DA}}{CSi_P}$$

the mass balance of detrital biogenic silica may be written as

$$\frac{dDSiO}{dt} = -k_{DSiO} DSiO + \frac{1}{CSi_P} \times [grazing_{ZL/DA} + sed_{DA}] \frac{DAF}{DA} - DSiO_{output}.$$

(d) *Oxygen in the water column*

$$\frac{dO}{dt} = Oair + photos - respiration + \frac{O_{diffus}}{watervol} - Onit_W + O_{input} - O_{output}.$$

Exchange between the air and the sea-surface has been calculated as a function of the concentration of saturated dissolved oxygen—$O_{sat} = f(T, S)$—and the wind speed (ws) according to the relation in Riley and Stefan (1988):

$$Oair = K_O (O_{sat} - O),$$

whereas the mass transfer coefficient, in h^{-1}, is given by

$$K_O = \frac{0.02671 + 2.13125 \times 10^{-4} ws^2}{z_{SG}},$$

ws is the wind speed (m/s), and d_1 is the thickness of first layer (1.0 m). The concentration of saturated oxygen (g/m^3) is calculated as a function of water temperature and salinity following the correlation from Aminot and Chaussepied (1983).

Oxygen photosynthesis, *photos*, is the function of phytoplankton and *Ulva* growth:

$$photos = photos_{PHY} + photos_U,$$

whereas the oxygen production by phytoplankton and *Ulva* may be written as

$$photos_{PHY} = Q_{PS} R_{PHY} \left(\frac{growth_F + growth_D}{CN_{PHY}} \right),$$
$$photos_U = \Psi growth_U.$$

Respiration of phytoplankton, zooplankton, bacteria, *Ulva* and shellfish is considered in the oxygen mass balance:

$$respiration = resp_{PHY} + resp_Z + resp_B + resp_U + resp_{SF},$$

whereas the different terms are calculated as

$$resp_{PHY} = R_{PHY} f_1(T) R_{PS} \left(\frac{DA + FL}{CN_{PHY}} \right),$$

$$resp_Z = R_Z f_1(T) R_{PS} \left(\frac{ZS + ZL}{CN_Z} \right),$$

$$resp_B = R_B f_1(T) upt_B,$$

$$resp_U = R_U f_{resp}(T) U.$$

The oxygen consumption in the water column due to nitrification can be expressed as

$$Onit_W = 0.064 Nitrif_W,$$

whereas 0.064 is the stoichiometric ratio, in $g\,O_2$/mmol N, for the respective reaction (Chapelle et al., 2000).

At the interface between the water column and the interstitial water, diffusion is responsible for *NO*, *NH*, *PO* and *O* fluxes (mmol/m^3 h). These fluxes can be represented as

$$NO_{diffus} = D_{NO} \frac{A_{SG}}{z_S} (SNO - NO)\beta,$$

$$NH_{diffus} = D_{NH} \frac{A_{SG}}{z_S} (SNH - NH)\beta,$$

$$PO_{diffus} = D_{PO} \frac{A_{SG}}{z_S} (SPO - PO)\beta,$$

$$O_{diffus} = D_O \frac{A_{SG}}{z_S} (SO - O)\beta,$$

whereas D_X are the sediment diffusion coefficients (m^2/h), A_{SG} refers to the interfacial area, in this case the total Sacca di Goro Area, z_S is the distance between the centers of the two layers, and β is the porosity (Chapelle et al., 2000).

A.6. Sediment equations

(a) *Nitrogen in the sediment*

$$\frac{dSNH}{dt} = (1 - \alpha_{denit}) Ndenit - Nitrif_S - \frac{NH_{diffus}}{interstvol} + Nmin_S \frac{partvol}{interstvol},$$

$$\frac{dSPN}{dt} = (sed_{PN1} + sed_{PN2}) \frac{watervol}{partvol} - Nmin_S.$$

Nitrification in the sediments, $Nitrif_S$, can be described as a first order process in ammonium concentration at the sediment:

$$Nnitrif_S = k_{nit} f_1(T) f_2(O) SNH,$$

whereas nitrate reduction can be expressed as a first order process in nitrate concentration at the sediment:

$$Ndenit = k_{denit} f_1(T) f_3(O) SNO.$$

According to Chapelle (1995) the mineralization flux in the sediments follows a first order equation dependent on temperature and oxygen concentration:

$$Nmin_S = k_{minN} f_1(T) f_4(O) SPN.$$

(b) *Phosphorous in the sediment*

$$\frac{dSPO}{dt} = -Padsorp + Pdesorp - \frac{PO_{diffus}}{interstvol} + Pmin \frac{partvol}{interstvol},$$

$$\frac{dSPA}{dt} = (Padsorp - Pdesorp) \frac{interstvol}{partvol},$$

$$\frac{dSPP}{dt} = (sed_{PP1} + sed_{PP2}) \frac{watervol}{partvol} - Pmin.$$

The mechanisms of adsorption and desorption may be represented as

$$Padsorp = k_{ads} \left(1 - \frac{SPA}{SPA_{max}} \right) SPO,$$

$$Pdesorp = k_{des} \frac{SPA}{SPA_{max}},$$

whereas the adsorption constant rate, k_{ads}, depend on the oxygen concentration in the sediment. When oxygen drops below 0.2 g/m^3 then anoxic conditions occur and the constant rate is reduced by a factor of five.

The phosphorous mineralization rate is expressed as

$$Pmin = k_{min\,P} f_1(T) f_4(O) SPP.$$

(c) *Oxygen in the sediment*

$$\frac{dSO}{dt} = -Omin_S - Onit_S - \frac{O_{diffus}}{interstvol}.$$

The oxygen consumption in the sediment is the sum of the consumption due to mineralization and nitrification, which can be expressed as

$$Omin_S = 0.212 Nmin_S,$$

$$Onit_S = 0.064 Nitrif_S,$$

whereas 0.212 and 0.064 are the stoichiometric ratios, in g O_2/mmol N, for the respective reactions (Chapelle, 1995).

Table 10
Nutrient and sediment parameters, from Lancelot et al. (2002) and Chapelle et al. (2000)

Parameters, computed quantities	Description	Value
k_{nit}	Nitrification rate at 0°C	$0.0083\,h^{-1}$
$f_1(T)$	$f_1(T) = \exp[k_T T]$	
k_T	Temperature increasing rate	$0.07°C^{-1}$
$f_2(O)$	$f_2(O) = \frac{SO}{K_{NitO} + SO}$	
K_{NitO}	Half-saturation coefficient for O_2 limitation of nitrification	$4.0\,g/m^3$
R_{UPC}	*Ulva* stoichiometric ratio	2.5 mg P/gdw
k_{DSiO}	Detrital silica dissolution constant	$7.5 \times 10^{-5}\,h^{-1}$
Q_{PS}	Photosynthetic ratio	1.5
R_{PHY}	Phytoplankton respiration rate at 0°C	$2.083 \times 10^{-3}\,h^{-1}$
ψ	Stoichiometric ratio	1.45 g O_2/gdw
R_{PS}	O_2 produced/N	0.212 g O_2/mmol
R_Z	Zooplankton respiration rate at 0°C	$3.5 \times 10^{-3}\,h^{-1}$
R_B	Bacteria respiration rate	$3.2 \times 10^{-3}\,h^{-1}$
R_U	Max. respiration rate	2.54×10^{-3} g O_2/(gdw h)
D_{NO}	Diffusion coefficient for nitrate in the sediment	$0.00072\,m^2/h$
D_{NH}	Diffusion coefficient for ammonium in the sediment	$0.00072\,m^2/h$
D_{PO}	Diffusion coefficient for phosphates in the sediment	$0.00072\,m^2/h$
D_O	Diffusion coefficient for oxygen in the sediment	$0.0036\,m^2/h$
A_{SG}	Sacca di Goro total surface	$2.7 \times 10^7\,m^2$
z_S	Distance between the centers of the two layers (water column and sediments)	0.8 m
β	Porosity	0.8
watervol	Water in the water column	$3.9 \times 10^7\,m^3$
interstvol	Interstitial water in the sediments	$2.1 \times 10^5\,m^3$
partvol	Volume of particles in the sediment (first cm)	$5.2 \times 10^4\,m^3$
k_{denit}	Denitrification rate at 0°C	$0.0125\,h^{-1}$
$f_3(O)$	$f_3(O) = 1.0 - \frac{SO}{K_{denitO} + SO}$	
K_{denitO}	Half-saturation coefficient for O_2 limitation of denitrification	$2.0\,g/m^3$
α_{denit}	Percentage of N denitrified into N_2	0.6
k_{minNW}	Nitrogen mineralization rate in water at 0°C	$0.00833\,h^{-1}$
k_{minN}	Benthic mineralization of organic N at 0°C	$0.00021\,h^{-1}$
$f_4(O)$	$f_4(O) = \frac{SO}{K_{min\,O} + SO}$	
K_{minO}	Half-saturation coefficient for O_2 limitation of mineralization	$0.5\,g/m^3$
k_{ads}	Adsorption rate oxic conditions $O_2 > 0.2\,g/m^3$	$8.33\,h^{-1}$
	Adsorption rate anoxic conditions $O_2 < 0.2\,g/m^3$	$1.67\,h^{-1}$
k_{des}	Desorption rate ($\mu g\,g^{-1}\,h^{-1}$)	$3.33\,h^{-1}$
k_{minP}	Benthic mineralization of organic *P* at 0°C	$0.00021\,h^{-1}$
SPA_{max}	Maximum *P* adsorption capacity for the sediment	685 μg/g

The functional forms of the nutrients and sediment model are described Table 10.

A.7. Shellfish equations

The filtering rates ($l\,h^{-1}$ individual^{-1}) are calculated according to Bacher et al. (1995) as

$$Filt_{SF} = [\alpha_{SF1} - \alpha_{SF2}(T - \alpha_{FH3})^2]W_{SH}^{\alpha_{SF4}}\alpha_{indiv}.$$

Total clam predation is the sum of the efficiency for each prey times its concentration, i.e.

$$grazing_{SF} = Filt_{SF}\sum eff_i C_i,$$

whereas oxygen consumption is given by

$$resp_{SF} = (\beta_{SF1} + \beta_{SF2}\beta_{SF3}^{T})W_{SF}^{\beta_{SF4}}\beta_{indiv}.$$

Individual clam excretion is the function of temperature and body dry weight. After multiplication by total number of individuals and a conversion factor (ε_{indiv}) will give the total amount of ammonium produced by shellfish:

$$reg_{SF} = (\varepsilon_{SF1} + \varepsilon_{SF2}T)W_{SF}^{\varepsilon_{SF3}}\varepsilon_{indiv}.$$

The shellfish model's parameters are described in Table 11.

Table 11
Shell fish parameters, from Chapelle et al. (2000), Bacher et al. (1995) and Dame (1993)

Parameters, computed quantities	Description	Value
α_{SF1}	Optimum filtration rate for a gdw individual	4.83 l/g/h
α_{SF2}	Filtration coefficient	0.013 l/g/h
α_{SF3}	Optimum temperature	19.0°C
α_{SF4}	Allometric coefficient	0.44
W	gdw per individual	0.083
eff_{POM}	Filtration efficacity coefficient for particulate organic matter	1
eff_{FL}	Filtration efficacity coefficient for flagellates	0.8
eff_{DA}	Filtration efficacity coefficient for diatoms	1
eff_{ZS}	Filtration efficacity coefficient for small zooplankton	1
eff_{B}	Filtration efficacity coefficient for bacteria	1
β_{SF1}	Respiration coefficient	0.43 mg O^2/h/gdw
β_{SF2}	Respiration coefficient	0.61 mg O_2/h/gdw
β_{SF3}	Respiration coefficient	1.04
β_{SF4}	Allometric coefficient	0.8
ε_{SF1}	Excretion rate at 0°C	14.7 g N/d/gdw
ε_{SF2}	Execretion coefficient	0.84
ε_{SF3}	Allometric coefficient	0.7

References

Aminot, A., Chaussepied, M., 1983. Manuel des méthodes d'analyses chimiques (RNO), CNEXO, 395pp.

Arhonditis, G., Tsirtsis, G., Angelidis, M.O., Karydis, M., 2000. Quantification of the effects of nonpoint nutrient sources to coastal marine eutrophication: application to a semi-enclosed gulf in the Mediterranean Sea. Ecological Modelling 129, 209–227.

Arnold, J.G., Allen, P.M., Bernhardt, G., 1993. A comprehensive surface-groundwater flow model. Journal of Hydrology 142, 47–69.

Bacher, C., Bioteau, H., Chapelle, A., 1995. Modelling the impact of a cultivated oyster population on the nitrogen dynamics: The Thau lagoon case (France). Ophelia 42, 29–54.

Barbanti, A., Cecherelli, V.U., Frascari, F., Rosso, G., Reggiani, G., 1992. Nutrient release from sediments and the role of bioturbation in the Goro Lagoon (Italy). Science of the Total Environment (Suppl.), 475–487.

Bartoli, M., Cattadori, M., Giordani, G., Viaroli, P., 1996. Benthic oxygen respiration, ammonium and phosphorus regeneration in surficial sediments of the Sacca di Goro (northern Italy) and two French coastal lagoons: a comparative study. Hydrobiologia 329, 143–159.

Bartoli, M., Nizzoli, D., Viaroli, P., Turolla, E., Castaldelli, G., Fano, E.A., Rossi, R., 2001. Impact of a Tapes philippinarum farming on nutrient dynamics and benthic respiration in the Sacca di Goro. Hydrobiologia 455, 203–212.

Bencivelli, S., 1998. La Dacca di Goro: La situazzione di emergenza dell'estate 1997. In: Lo stato dell'ambiente nella provincia di Ferrara. Anno 1997. Amministrazione Provinciale di Ferrara, Servizio Ambiente, pp. 61–66.

Billen, G., 1991. Protein degradation in the aquatic environment. In: Chrost, R. (Ed.), Microbial Enzymes in the Aquatic Environment, Vol. 7. Springer, Berlin, pp. 123–143.

Cattaneo, E., Zaldívar, J.M., Murray, C.N., Viaroli, P., Giordani, G., 2001. Application of LOICZ methodology to a Mediterranean Coastal Lagoon: Sacca di Goro (Italy). EUR Report no. 19921, European Commission, JRC-Ispra, Italy.

Ceccherelli, V.U., Riggiani, G.C., Caramori, G., Giaiani, V., Corazza, C., 1994. Le comunità macrobentoniche della Sacca di Goro e gli effetti di disturbo ambientale: Risultate di due anni d'indagine (Dicembre 1987–Dicembre 1989). In: Bencivelli, S., Castaldi, N., Finessi, D. (Eds.), Sacca di

Goro: Studio integrato sull'ecologia. Provincia di Ferrara, FrancoAngeli, Milano, pp. 83–108.

Chapelle, A., 1995. A preliminary model of nutrient cycling in sediments of a Mediterranean lagoon. Ecological Modelling 80, 131–147.

Chapelle, A., Ménesguen, A., Deslous-Paoli, J.M., Souchu, P., Mazouni, N., Vaquer, A., Millet, B., 2000. Modelling nitrogen, primary production and oxygen in a Mediterranean lagoon. Impact of oysters farming and inputs from the watershed. Ecological Modelling 127, 161–181.

Ciavola, P., Gonella, M., Tessari, U., Zamariolo, A., 2000. Contributo alla conoscenza del clima meteomarino della Sacca di Goro: misure correntometriche e mareografiche. Studi Costieri 2, 153–173.

Cioffi, F., Di Eugebio, A., Gallerano, F., 1995. A new representation of anoxic crisis in hypertrophic lagoons. Applied Mathematical Modelling 19, 685–695.

Colombo, G., Bisceglia, R., Zaccaria, V., Gaiani, V., 1994. Variazioni spaziali e temporali delle caratteristiche fisico-chimiche delle acque e della biomassa fitoplantonica della Sacca di Goro nel quadriennio 1988–1991. In: Bencivelli, S., Castaldi, N., Finessi, D. (Eds.), Sacca di Goro: Studio integrato sull'ecologia. Provincia di Ferrara, FrancoAngeli, Milano, pp. 9–82.

Dalsgaard, T., Nielsen, L.P., Brotas, V., Viaroli, P., Underwood, G., Nedwell, D., Sundbäck, K., Miles, A., Bartoli, M., Welssh, D., Dong, L., Cooper, M., Thornton, D.C.O., Ottosen, L.D.M., Carbirita, M.T., Serôdio, J., Castaldelli, G., Göransson, E., Risgaard-Petersen, N., 1999. Denitrification in shallowcoastal European waters: a synthesis of the NICE project. Proceedings of the ELOISE (European Land-Ocean Interaction Studies) Third Open Science Meeting, Noordwijkerhout, The Netherlands, 1–4 December 1999.

Dame, R.F. (Ed.), 1993. Bivalve filter-feeders in estuarine and coastal ecosystem processes. NATO ASI Series, Vol. 33. Springer, Berlin.

De Wit, R., Stal, L.J., Lomstein, B.A., Herbert, R.A., van Gemerden, H., Viaroli, P., Cecherelli, V.U., Rodriguez-Valera, F., Bartoli, M., Giordani, G., 2001. ROBUST: The ROle of BUffering capacities in STabilising coastal lagoon ecosystems. Continental Shelf Research 21, 2021–2041.

Ferrari, I., Carrieri, A., Gaiani, V., 1994. Ricerche sullo zooplancton della Sacca di Goro (Novembre 1988–Ottobre 1989). In: Bencivelli, S., Castaldi, N., Finessi, D. (Eds.), Sacca di Goro: Studio integrato sull'ecologia. Provincia di Ferrara, FrancoAngeli, Milano, pp. 131–154.

Giordani, G., Bartoli, M., Cattadori, M., Viaroli, P., 1996. Sulphide release from anoxic sediments in relation to iron availability and organic matter recalcitrance and its effects on inorganic phosphorus recycling. Hydrobiologia 329, 211–222.

Harzallah, A., Chapelle, A., 2002. Contribution of climate variability to occurrences of anoxic crises "malaïgues" in the Thau lagoon (Southern France). Oceanologica Acta 25, 79–86.

Herut, B., Krom, M., 1996. Atmospheric input of nutrients and dust to the SE Mediterranean. In: Guerzoni, S., Chester, R. (Eds.), The Impact of Desert Dust Across the Mediterranean. Kluwer, Dordrecht, pp. 349–358.

Kjerfve, B., 1994. Coastal Lagoon Processes. Elsevier Science Publishers, Amsterdam, xx + 577pp.

Lancelot, C., Le Roy, D., Billen, G. (Eds.), 1991. The dynamics of *Phaeocystis* blooms in nutrient enriched coastal zones of the channel and the North Sea. Third annual progress report.

Lancelot, C., Staneva, J., Van Eeckhout, D., Beckers, J.M., Stanev, E., 2002. Modelling the Danube-influenced northwestern continental shelf of the Black Sea. II. Ecosystem response to changes in nutrient delivery by the Danube river after its damming in 1972. East Coastal Shelf Science 54, 473–499.

Luyten, P. (Ed.), 1999. COHERENS—dissemination and exploitation of a coupled hydrodynamical-ecological model for regional and shelf seas, MAS3-CT97-0088. Final Report. MUMM Internal Report, Management Unit of the Mathematical Models.

Medinets, M., 1996. Shipboard derived concentrations of sulphur and nitrogen compounds and trace metals in the Mediterranean aerosol. In: Guerzoni, S., Chester, R. (Eds.), The Impact of Desert Dust Across the Mediterranean. Kluwer, Dordrecht, pp. 359–368.

Milan, C., 1999. Indagini in Sacca di Goro per valutare gli effetti prodotti dagli eventi alluvionale del Novembre 1994. Relazione sull'attività di monitoragio chimico e microbiologico (1997–1998). ARPA.

O'Kane, J.P., Suppo, M., Todini, E., Turner, J., 1992. Physical intervention in the lagoon Sacca di Goro. An examination using a 3-D numerical model. Science of the Total Environment (Suppl.), 489–509.

Okubo, A., 1971. Oceanic diffusion diagrams. Deep-Sea Research 18, 789–802.

Piccoli, F., Godini, E., 1994. Ricerche qualitative e quantitative sulla vegetazione della Sacca di Goro anni 1989–1990. In: Bencivelli, S., Castaldi, N., Finessi, D. (Eds.), Sacca di Goro: Studio Integrato Sull'ecologia. Provincia di Ferrara, FrancoAngeli, Milano, pp. 227–243.

Pugnetti, A., Viaroli, P., Ferrari, I., 1992. Process leading to dystrophy in a Po River Delta lagoon (Sacca di Goro): phytoplankton-macroalgae interactions. Science of the Total Environment (Suppl.), 445–456.

Riley, M.J., Stefan, H., 1988. MINLAKE: A dynamic lake water quality simulation model. Ecological Modelling 43, 155–182.

Sei, S., Rossetti, G., Villa, F., Ferrari, I., 1996. Zooplankton variability related to environmental changes in a eutrophic coastal lagoon in the Po Delta. Hydrobiologia 329, 45–55.

Solidoro, C., Brando, V.E., Dejak, C., Franco, D., Pastres, R., Pecenik, G., 1997a. Long term simulations of population dynamics of *Ulva r.* in the lagoon of Venice. Ecological Modelling 102, 259–272.

Solidoro, C., Pecenik, G., Pastres, R., Franco, D., Dejak, C., 1997b. Modelling macroalgae (*Ulva rigida*) in the Venice

lagoon: model structure identification and first parameters estimation. Ecological Modelling 94, 191–206.

Taylor, G.I., 1953. Dispersion of soluble matter in solvent slowly flowing through a tube. Proceedings of the Royal Society of London A219, 186–203.

Tusseau, M.-H., Lancelot, C., Martin, J.M., Tassin, B., 1997. 1-D coupled physical-biological model of the northwestern Mediterranean Sea. Deep-Sea Research II 44, 851–880.

Tusseau, M.-H., Mortier, L., Herbaut, C., 1998. Modeling nitrate fluxes in an open coastal environment (Gulf of Lions): transport versus biogeochemical processes. Journal of Geophysical Research 103, 7693–7708.

Viaroli, P., Pugnetti, A., Ferrari, I., 1992. *Ulva rigida* growth and decomposition processes and related effects on nitrogen and phosphorus cycles in a coastal lagoon (Sacca di Goro, Po River Delta). In: Colombo, G., Ferrari, I., Ceccherelli, V.U., Rossi, R. (Eds.), Marine Eutrophication and Population Dynamics. Olsen & Olsen, Fredensborg, pp. 77–84.

Viaroli, P., Pugnetti, A., Naldi, M., Zaccaria, V., 1994. Ricerche sul fitoplancton e su crescita e decomposizione di Ulva Rigida nella Sacca di Goro. In: Bencivelli, S., Castaldi, N., Finessi, D. (Eds.), Sacca di Goro Studio integrato sull'ecologia. Provincia di Ferrara, FrancoAngeli, Milano, pp. 109–130.

Viaroli, P., Bartoli, M., Bondavalli, C., Naldi, M., 1995. Oxygen fluxes and dystrophy in a coastal lagoon colonized by *Ulva rigida* (Sacca di Goro, Po River Delta, Northern Italy). Fresenius Environment Bulletin 4, 381–386.

Viaroli, P., Azzoni, R., Bartoli, M., Giordani, G., Tajé, L., 2001. Evolution of the trophic conditions and dystrophic outbreaks in the Sacca di Goro lagoon (Northern Adriatic Sea). In: Faranda, F.M., Guglielmo, L., Spezie, G. (Eds.), Structure and Processes in the Mediterranean Ecosystems. Springer, Milano, Italia, pp. 443–451 (Chapter 56).

Yanagi, T., 2000. Coastal Oceanography. Kluwer Publishers, Dordrecht.